Journal of Archaeological Science: Reports 33 (2020) 102543

Contents lists available at ScienceDirect

Journal of Archaeological Science: Reports

journal homepage: www.elsevier.com/locate/jasrep

The lowland Maya settlement landscape: Environmental LiDAR and ecology

Whittaker Schroder[a,*], Timothy Murtha[a], Charles Golden[b], Armando Anaya Hernández[c], Andrew Scherer[d], Shanti Morell-Hart[e], Angélica Almeyda Zambrano[a], Eben Broadbent[a,f], Madeline Brown[g]

[a] Center for Latin American Studies, Florida Institute for Built Environment Resilience, The University of Florida, Gainesville, FL 32611, USA
[b] Department of Anthropology Brandeis University, 415 South St., Waltham, MA 02454, USA
[c] Center for Sustainable Development Studies and Conservation of Wildlife (CEDESU), Universidad Autónoma de Campeche, Mexico
[d] Department of Anthropology, Brown University, Box 1921, Providence, RI 02912, USA
[e] CNH534, Department of Anthropology, McMaster University, 1280 Main St. West, Hamilton, ON L8S4L9, Canada
[f] School of Forest Resources and Conservation, University of Florida, Gainesville, FL 32611, USA
[g] Department of Anthropology, University of Maryland, 1111 Woods Hall, 4302 Chapel Ln., College Park, MD 20742, USA

ARTICLE INFO

Keywords:
LiDAR
GIS
Settlement patterns
Mesoamerica
Maya
Regional survey

ABSTRACT

This paper presents the archaeological evaluation of 458 tiles of LiDAR collected by environmental scientists over southern Mexico using the G-LiHT system of NASA's Goddard Space Flight Center. Specifically, this article describes the results of a full processing, inspection, and annotation of these data for the identification and baseline analysis of archaeological features. In this paper, we: 1) introduce the dataset and describe our efforts to systematically process and annotate archaeological features and 2) revisit the cultural and ecological context of the samples. The results presented here confirm some of the conclusions presented previously, including the benefit of mining large previously acquired digital data for archaeological information, the diversity of lowland settlement and features in between areas already well-documented, and the contribution to landscape archaeology of such transect samples when coupled to macro-environmental data sets. These data also fill in some details about the prehispanic Mesoamerican landscape, raising new questions about the relationship between past settlements and regional cultural, political, and ecological systems. Finally, these data offer important foundational inventories for discussing how to preserve and conserve archaeological resources across the lowlands, especially when these resources are not tied to monumental architecture.

1. Introduction

In this article, we present a full archaeological inventory, description, and regional analysis of LiDAR transects collected by NASA Goddard's LiDAR, Hyperspectral, and Thermal Imager (G-LiHT) team and collaborating environmental scientists over the Maya lowlands. Building on an earlier reanalysis of environmental LiDAR data for archaeology in Mesoamerican applications and implications (Golden et al., 2016), we: 1) describe the full inventory of archaeological features provisionally identified through visual analysis, and 2) discuss how these data compare to the known archaeological, ecological, and modern land use and conservation context. These results, together with a growing body of research using archived LiDAR data (Davis et al., 2019a, 2019b; Dunning et al., 2019; Fernández-Diaz and Cohen, 2020; Johnson and Ouimet, 2014; Liebmann et al., 2016; Ruhl et al., 2018), further confirm that LiDAR collected for conservation, development, or emergency response purposes offer as yet underutilized resources in the Neotropics for contributing to archaeological understandings of variations in prehispanic landscapes, land-use systems, and settlement patterns.

Dedicated archaeological airborne LiDAR collection and analyses of select regions of the lowlands have provided robust samples for the quantification of archaeological feature numbers and densities in discrete areas of the Maya region (Canuto et al., 2018; Chase et al., 2010, 2011, 2012, 2014a, 2014b; Ebert et al., 2016; Hutson, 2015; Magnoni et al., 2016; Stanton et al., 2020). While transformative, this research tends to cover relatively homogenous areas in terms of ecology, hydrology, and geology, and furthermore, discrete study areas may be separated by extensive spatial gaps. The G-LiHT data offer important alternative, complementary, and freely available resources concerning archaeological settlement patterns and past land use along a combined transect of 3,200 km. Critically, although these data do not provide

* Corresponding author.
E-mail address: wschroder@ufl.edu (W. Schroder).

https://doi.org/10.1016/j.jasrep.2020.102543
Received 17 July 2020; Received in revised form 20 August 2020; Accepted 21 August 2020
Available online 19 September 2020

wide-coverage in any single region, they do intersect with multiple ecoregions, ecological systems, drainage basins, and geological formations across southern Mexico. These data expand our perceptions beyond largely site-focused interpretations (Golden et al., 2016) and analyses derived from more typical comparative site descriptions (Murtha, 2015). Here we argue G-LiHT survey data provide a more representative perspective on the diversity, density, complexity, and patterning of the spatial distribution of archaeological features across the lowlands. These multi-regional data are especially useful when compared to other macro datasets (e.g., Beach et al., 2015; FAO, 2012; Fick and Hijmans, 2017; INEGI, 2000, 2010), such as those highlighting variability in ecological systems across the lowlands. Using extensive G-LiHT data, we have investigated which ecological factors contributed to relatively higher density settlement and whether those areas of density were also located primarily around monumental ceremonial centers and known sites. Moreover, we begin to address how settlement patterns and other anthropogenic features covary with one another alongside other ecological factors across the Maya lowlands.

Initial observations resulting from these analyses and reported here support the argument presented by other scholars that not all densified Maya settlements are accompanied by monumental and centralized architecture and that regional physical patterning of settlements in some areas does not appear to reflect a strongly hierarchical premodern Maya political system (Arnauld et al., 2013; Lemonnier and Vannière, 2013; Nondédéo et al., 2013). We also observe diversity in the scale, intensity, and distribution of landesque features not necessarily associated with political evolutionary models that link intensification to central political authority. We conclude that among the variables analyzed, known archaeological site location, physiographic region, and modern precipitation patterns are the strongest predictors for feature density. While ecological variables influenced the location of archaeological features, the results were less predictable and require more localized analysis. Raising these observations here generates a whole series of questions about the ancient Maya landscape we aim to investigate in follow up studies.

The resolution of the G-LiHT data is also sufficient to examine distribution patterns of the destruction of archaeological resources, with the potential to contribute to conservation planning in relation to modern development and looting. While we do not offer solutions in this paper, future archaeological conservation design and planning efforts would benefit from a review of these data. For example, we clearly demonstrate that the threats to the conservation of some of these archaeological features in relation to modern land use, protected lands, and urban areas are not likely to be driven by concerns for monumental architecture but a landscape history consistently challenged by infrastructure development. These results encourage us to think more broadly about the important research partnerships that can emerge from these studies, especially those focused on remote sensing, planning, future land use management, and conservation.

2. LiDAR applications in Mesoamerican archaeology

Over the past decade, LiDAR has become a primary tool for archaeological survey in regions worldwide, with revolutionary promise in forested areas in Mesoamerica (Ainsworth et al., 2013; Arnott and Maki, 2019; Banaszek, 2020; Barnes, 2003; Beach et al., 2019; Bedford et al., 2018; Beex, 2017; Benjamin et al., 2018; Bernardini et al., 2013; Bewley et al., 2005; Brewer et al., 2017; Canuto et al., 2018; Carson et al., 2014; Chase et al., 2011, 2012, 2014a, 2014b; Chase and Chase, 2017; Chevance et al., 2019; Comer et al., 2019; Doneus et al., 2008; Evans and Fletcher, 2015; Fernández-Diaz et al., 2014; Fisher et al., 2017, 2016, 2011; Fisher and Leisz, 2013; Henry et al., 2019; Hightower et al., 2014; Horn and Ford, 2019; Inomata et al., 2017, 2018, 2019, 2020; Jones and Bickler, 2017; Liebmann et al., 2016; Masini et al., 2011; McFarland and Cortes-Rincon, 2019; McKee et al., 1994; Reese-Taylor et al., 2016; Rosenswig et al., 2013; Sheets and Sever, 1988; Sheets, 1991; Sheets et al., 1991; von Schwerin et al., 2016; Yaeger et al., 2016). LiDAR has proven useful for site survey, site interpretation, site delineation, and especially site discovery, building off earlier regional and remote sensing approaches in Maya archaeology (Ashmore, 1984, 1981; Beach et al., 2015; Dunning, 1996; Dunning and Beach, 2010; Fedick, 1996; Garrison, 2010; Garrison et al., 2008, 2011). The majority of these LiDAR data have been captured using airborne systems and are not linked to other remote sensing products. More recently, LiDAR systems mounted on drones have also proven their efficacy (Barbour et al., 2019; Murtha et al., 2019a; Risbøl and Gustavsen, 2018; VanValkenburgh et al., 2020).

LiDAR has the potential to provide full coverage mapping of above surface archaeological features, especially in densely forested zones where traditional ground-based survey is impractical in terms of labor cost and time (Balkansky et al., 2000; Falconer and Savage, 1995; Kolb and Snead, 1997; Kowalewski, 1990; Parsons, 1990; Plog, 1990; Sanders, 1999; Sanders and Santley, 1983; Terrenato and Ammerman, 1996; Underhill et al., 2002; Wilkinson, 2000), and has been used to highlight how quickly these archaeological landscapes are disappearing (de Matos Machado and Hupy, 2019; Kincey et al., 2008; Kincey and Challis, 2010; Megarry et al., 2016; Roberts et al., 2017). LiDAR survey captures a static moment of dynamic, constantly changing landscapes, so no matter how extensive or critically important, full coverage LiDAR mapping offers a regional and incomplete perspective. The data presented here point us toward identifying ways to improve and scale up regional observations or at least identify gaps in our approaches for the design of future research.

To date, approaches to capture LiDAR data across a large region, as with efforts in western Belize (Chase et al., 2011, 2014b; Horn and Ford, 2019; Yaeger et al., 2016), Petén, Guatemala (Canuto et al., 2018), and Yucatán, Mexico (Hare et al., 2014; Hutson, 2015; Magnoni et al., 2016; Stanton et al., 2020) have transformed basic assumptions about settlement density and the scale of landscape modification within discrete mission regions. Yet, while the scale of the largest sample regions encompasses thousands of square kilometers, archaeologists have yet to combine these data to conduct inter- and super-regional analysis. In some sense, LiDAR collected by the 2013 G-LiHT mission in Mexico acts as a data corridor and offers an opportunity to fill gaps between discrete LiDAR datasets collected by individual research teams, while rescaling and investigating archaeological feature form and distribution across the lowland geography.

Commonly, archaeological and anthropological questions may be answered using datasets relevant to research in numerous allied disciplines. Over the last two decades, the value of interdisciplinary approaches has become increasingly evident in archaeological publications that include ecologists and other allied scientists (Beach et al., 2003, 2006, 2008, 2009, 2011; Dunning, 1996, 1997; Dunning and Beach, 2004; Dunning et al., 1992, 1994, 1998, 1999, 2002; Fedick, 1994, 1996; Fedick and Ford, 1990; Gómez-Pompa et al., 2003; Murtha et al., 2018, 2019b; Sanders, 1962, 1963, 1973, 1977; Scarborough et al., 2012a, 2012b). LiDAR is appropriate to address questions in a variety of fields, including archaeology, anthropology, sociology, geography, ecology, and others. While expensive to acquire, LiDAR has broad scientific value for interdisciplinary research within and beyond archaeology, also highlighting the importance of the scientific distribution of such data as opposed to extended embargos. Rapid release of LiDAR datasets allows for collaborations between research projects, especially since these data can be used to address a broad range of contemporary issues related to land use, environmental degradation, and climate change. Moreover, LiDAR datasets have additional value as they document landscapes at particular moments in time, useful for scholars interested in questions of diachronic change.

3. LiDAR data collection

The data used in this study were collected by the NASA Goddard Space Flight Center, led by Dr. Bruce Cook, using NASA Goddard's

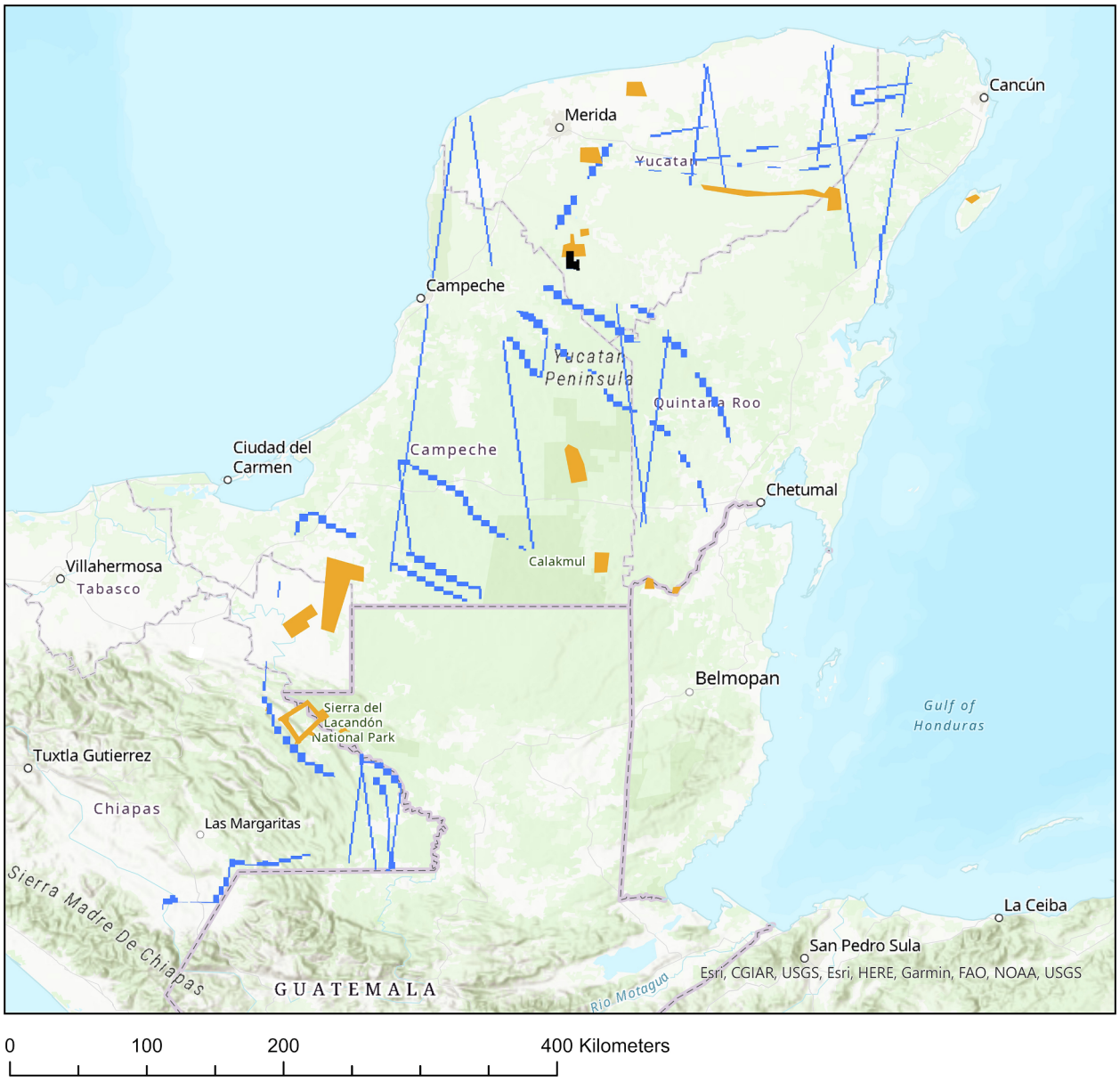

Fig. 1. Map of all G-LiHT samples analyzed in this paper (blue) and unanalyzed Kiuic samples (dark blue) compared to location and extent of other proximate LiDAR survey extents (orange) from southern Mexico. Samples are redrawn from (Fernández-Diaz, 2019; Hare et al., 2014; Hutson et al., 2016; Inomata et al., 2018; Stanton et al., 2020).

LiDAR, Hyperspectral & Thermal Imager (G-LiHT) system (Cook et al., 2013; Golden et al., 2016; Hernández-Stefanoni et al., 2015). The primary objective of the mission was to refine measurements of above-ground forest carbon stocks in Mexico (see Golden et al., 2016: Fig. 1). The full background of the instruments and the original source of data is summarized in a previous article (Golden et al., 2016), so we provide only an abbreviated summary here. The data analyzed for this study were collected in April of 2013 as part of a multi-institutional, bi-national study of above-ground biomass (AGB) and species-richness that covered large swaths of Mexico (Hernández-Stefanoni et al., 2015). The research was designed to inform deforestation programs, including the United Nations REDD+ (Reducing Emissions from Deforestation and forest Degradation, plus conservation, sustainable management of forests and enhancement of forest carbon stocks), and to aid in the design of effective strategies for selecting natural protected areas (see http://www.un-redd.org/aboutredd).

The key instrument employed for this mission was G-LiHT, a multi-sensor airborne imaging system that includes LiDAR, Imaging Spectrometer, and Thermal instrument intended to map simultaneously the composition, structure, and function of terrestrial ecosystems (see Cook et al., 2013 for full details). The airborne laser scanning (ALS) instrument of G-LiHT is a VQ-480 (Riegl USA, Orlando, FL, USA), which includes a high-performance laser rangefinder and a rotating polygon mirror with three facets to deflect a 1550 nm Class 1 laser beam onto the ground. Three-dimensional LiDAR returns and user-friendly data products (see Cook et al., 2013) are openly distributed through the G-LiHT Data Center Webmap (http://G-LiHT.gsfc.nasa.gov).

610 LiDAR samples were captured and processed over southern Mexico, ranging in extent from 3 ha to 4100 ha (Golden et al., 2016). Our previous study documented the promise of these data for archaeological research, their value derived especially from the sampling of diverse types of ecological settings, land-use regimes, and modern infrastructure along north–south and east–west transects across much of the lowlands (Golden et al., 2016). Our focus in undertaking analyses of these data is not centered on site discovery or identification; instead, our effort expands site-based interpretations of the relationship between ancient Maya cities, settlement patterns, and their broader landscape and environmental contexts. We are especially interested in

Table 1
Raw counts of features annotated in 458 tiles, with modified definitions (Ashmore, p. 40, 2007; Canuto et al., 2018; Stanton et al., 2020). Counts of linear features refer to individual line segments; length is a more useful statistic.

Feature Type	Definition	Count	Measurement
Polygonal			**Area (ha)**
Structures	Architecture, including buildings and superstructures not supporting other visible constructed features	54,488	441.22
Platforms	Basal substructure supporting one or more other structures	3,244	259.99
Plazas	Sunken or elevated pavement enclosed by structures on 1 or more sides or a level area enclosed by structures on 3 or more sides	3,659	121.99
Causeways	Inter- and intra-site elevated roads	4	0.81
Aguadas/Borrow pits	Excavated area, used for collecting building material and/or water	2,731	43.52
Polygonal Subtotal		**64,126**	**867.54**
Linear			**Length (km)**
Architectural terraces	Rectilinear features built into hillsides or summits to support architecture, i.e. platforms with fewer than 4 constructed sides	2,350	122.7
Agricultural terraces	Contour, footslope, and box terracing on hillslopes	8,763	432.5
Other possible agricultural terraces	Ambiguous terrace features on steep slopes or in low ground point density areas	1,476	92.9
Canals/Ditches	Excavated linear features, sometimes associated with low-lying wetlands or bodies of water	335	35.5
Paths	Indented linear features produced by walking	392	94.4
Walls	Freestanding, additive linear features	10,287	700.9
Linear Subtotal		**23,603**	**1,478.9**
Total		**87,729**	

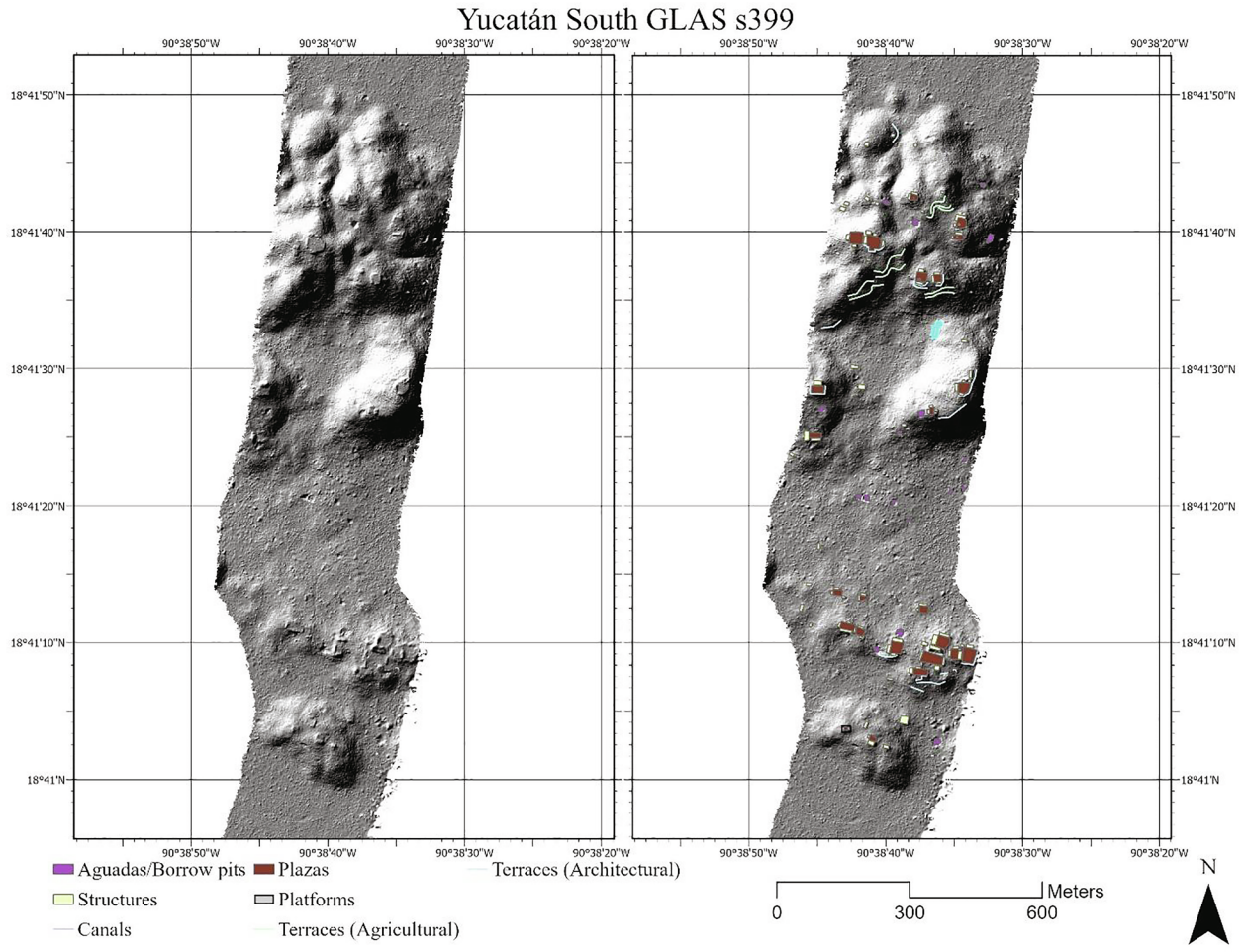

Fig. 2. Hillshade of Yucatán South GLAS s399 tile illustrating examples of architectural terraces at hill summits and agricultural terraces along midslopes and footslopes. Annotated version on the right.

what the spatial distribution of anthropogenic feature data can tell us about the variability in choices made by the prehispanic Maya to modify their landscapes in relation to variables including population density, political history, and other ecological and environmental factors. Our research quantifies interregional variability rather than interpreting how a single sample or subset of samples can be used to investigate a particular site. Since few archaeological sites were completely surveyed by the G-LiHT transects, these data do not provide the detail to fully assess settlement patterns at a single site. Moreover, these data, like all remote sensing data, lack information regarding site chronology. Their benefit lies in the linear extent of the survey that facilitates analysis of variability in the form and distribution of Maya

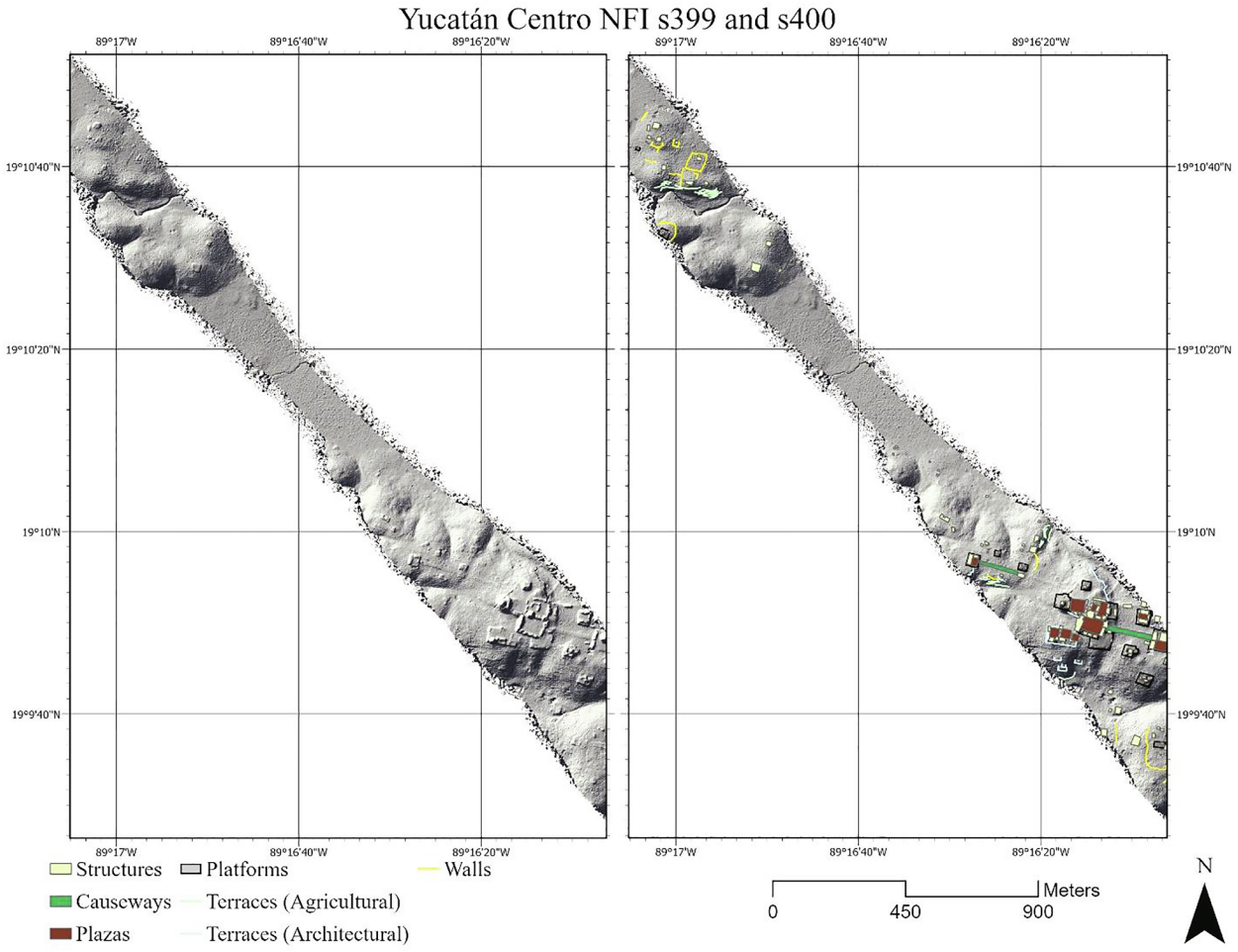

Fig. 3. Hillshade of Yucatán Centro NFI s399 and s400 tiles illustrating a diversity of feature types in upland areas. Annotated version on the right.

settlements across regional ecological systems and, when coupled with archaeologically derived chronological data, through time.

The G-LiHT survey transects cover a landscape shaped by more than 7,000 years of agrarian activity, rural settlement, and urbanization processes (Inomata et al., 2013, 2020; McClung de Tapia, 1992; Piperno et al., 2009). Importantly, these flight tiles connect well-sampled areas such as the Central Maya lowlands with western regions like the Usumacinta River basin that have been more sparsely surveyed (Fig. 1) (Golden et al., 2016). They also connect coastal sites to landlocked upland sites reliant on rainfed agriculture throughout their history. In our previous paper, we documented the important structure and variety of these samples and why they are unique and important to studies in the Maya lowlands (Golden et al., 2016).

We revisit these data here to provide a more complete contextual analysis of the flight samples, including visual annotation of 458 tiles from the core region of our study area, focusing exclusively on samples within the Maya area, east of the Isthmus of Tehuantepec. These samples vary in size but typically measure 7 km long by 300 m wide and cross the states of Quintana Roo, Yucatán, Campeche, Tabasco, and eastern Chiapas, with some of the Chiapas flight paths extending into parts of Petén, Guatemala. A targeted and gridded area of coterminous flight transects within the municipality of Oxkutzcab (near the archaeological site of Kiuic) was omitted from this study due to a specific sampling strategy for those samples that diverges with the single flight tiles analyzed here (George-Chacón et al., 2019; Hernández-Stefanoni et al., 2014, 2015, 2018). The total sampled area annotated and analyzed covers a flight length of approximately 3,200 km and an area of 1,118 square kilometers, omitting overlapping portions of tiles. Across all tiles, the nominal ground point density was 3.7 points per square meter, with a range between 0.3 and 11.0. Fewer than 6% of tiles (primarily located in Chiapas) had ground point densities below 1 point per square meter; a value cited as sufficient to document archaeological features in Neotropical Mesoamerica (Rosenswig et al., 2013, p. 1497).

4. Annotation of the flight paths

This study reports on the second phase of an iterative analysis, relying on visual identification and recording of archaeological features and a preliminary examination of feature data as they relate to various environmental, geographic, and contextual variables. Further analysis of the LiDAR data and ground verification are the long-term goals of our research. The questions we ask here are at a landscape scale, and due to the large spatial scale of the data, minor errors in the feature data reported here are not expected to alter our initial observations and conclusions significantly. Similarly, we cannot account for changes to the archaeological landscape that are now obscured by modern settlement. We have scaled our interpretations to account for potential errors that we cannot address methodologically.

Researchers have experimented with a diverse array of LiDAR processing and visualization techniques in Mesoamerican archaeology (Canuto et al., 2018; Chase and Chase, 2017; Chiba et al., 2008; De Reu et al., 2013; Horn and Ford, 2019; Hutson, 2015; Inomata et al., 2018; Kokalj et al., 2010, 2011; Kokalj and Somrak, 2019; Magnoni et al., 2016; Pingel et al., 2015; Zakšek et al., 2011). To streamline consistent application across tiles and to avoid the misidentification of false positives due to technical artifacts, we developed digital elevation models

Table 2
Density data for all 458 flight paths categorized by equal quantile (20%) intervals.

Quantile	Density Category	Structures and Platforms per Ha	Ha per Structure and Platform
Top 20%	Very High	0.93–3.75	0.27–1.08
	High	0.52–0.93	1.08–1.92
	Medium	0.21–0.52	1.92–4.76
	Low	0.02–0.21	4.76–50
Bottom 20%	Very Low	0–0.02	greater than50

(DEM) relying on basic processing, reported ground points, and standardized single hillshades overlaid with the derived DEM at 50% transparency as a baseline visualization. While we used ArcGIS Pro 2.4, any recent desktop GIS software, including opensource software such as GRASS, QGIS, and gvSIG can replicate our results.

We documented five distinct, durable feature types as polygons: 1) structures, 2) platforms, 3) plazas, 4) *aguadas* or borrow pits, and 5) causeways; and five distinct feature types as polylines: 1) architectural terraces, 2) agricultural terraces, 3) walls, 4) canals or ditches, and 5) paths. Conforming to decades of standards (see Ashmore, 1981, 1984; Ashmore, p. 40, 2007; Becker, 1982), we defined features according to the basic definitions summarized in Table 1. In most cases, we did not attempt to assign a function to these features, except for terraces where we distinguished between architectural and agricultural uses, relying on core definitions of terracing identified and agreed upon throughout the Maya lowlands (see Donkin, 1979; Dunning, 1996; Fedick, 1988; Murtha, 2009; Neff, 2008) (Figs. 2–3). Some agricultural terraces in Chiapas were further subdivided; these possible terraces are difficult to interpret solely through remote methods because they are found in areas with low ground point densities, with steep slopes, and distant from other archaeological features and settlements. Further field investigation is needed before we include them in analyses at this scale. Modern reservoirs, roads, and paths, verified as contemporary using available ortho imagery, were not annotated as archaeological features.

Linear, freestanding walls are common throughout the study area, and given their variety of potential uses, we made no functional interpretations (Hutson et al., 2007; Hutson, 2017). These features have been documented across the lowlands and offer a diversity of formal functions, including for agriculture (Turner, 1974), defense (e.g., Demarest et al., 1997; Palka, 2001; Rice and Rice, 1981; Scherer and Golden, 2009; Webster et al., 2007), intracommunity subdivision (e.g., Hare and Masson, 2012; Hare et al., 2014; Hutson et al., 2006; Kintz, 1983; Magnoni et al., 2014), and to support informal land-use boundaries, sometimes as a side effect of clearing areas for cultivation or construction (Abrams, 1994; Bullard, 1952; LeCount et al., 2019). The majority of walls are dry-laid stone, known as *albarradas* across much of the Yucatán peninsula (Alexander, 1999; Cain, 2019; Magnoni et al., 2012). Walls are potentially more difficult to identify or isolate as archaeological because they persist over long periods of time and may still be in use today.

Not surprising, given their visibility on the surface, structures and platforms make up the majority of features annotated across the

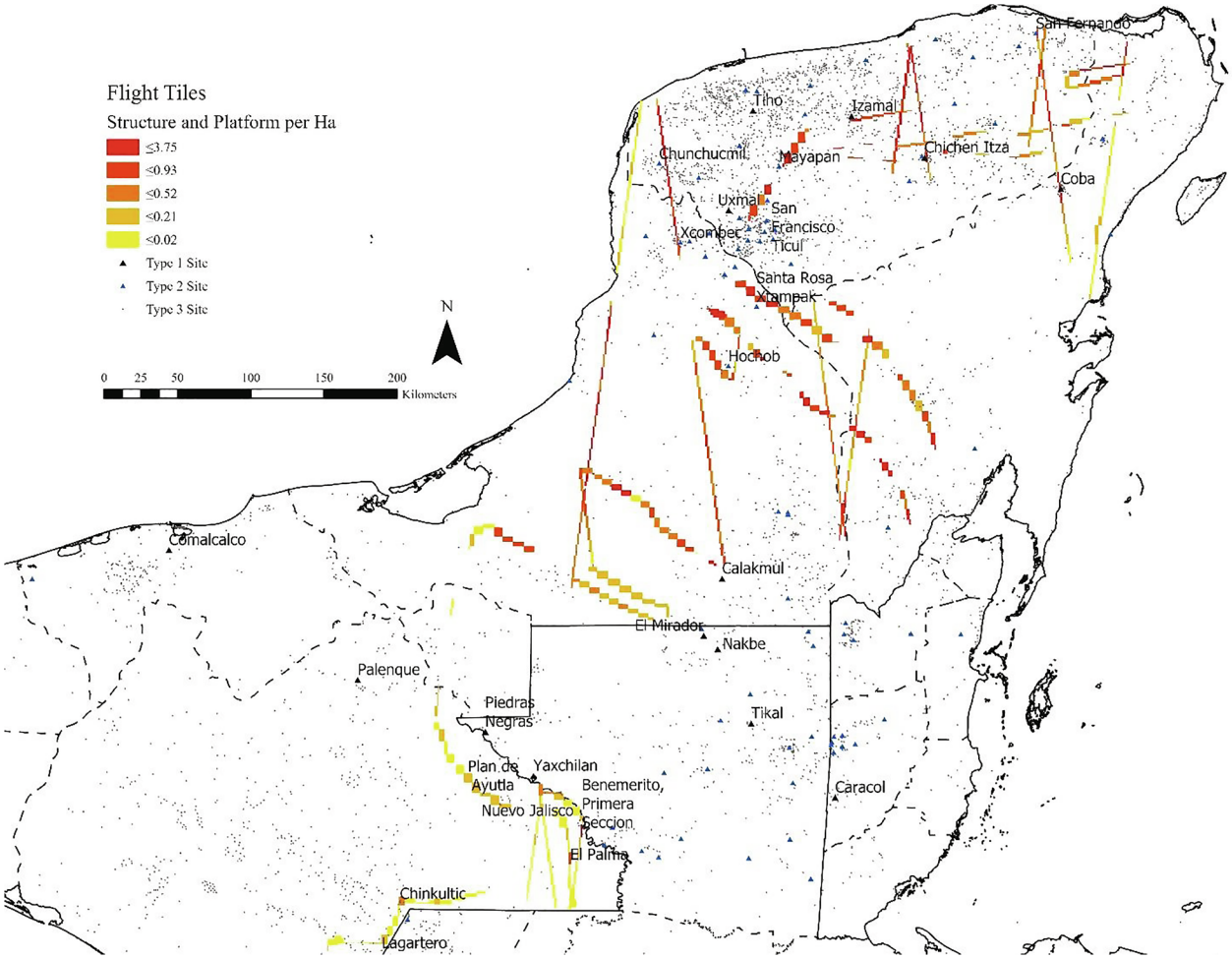

Fig. 4. Map of structure and platform density by flight path with Witschey and Brown (2010) sites and other sites mentioned in the text. Density categories in count per ha and ha per count compiled in Table 2.

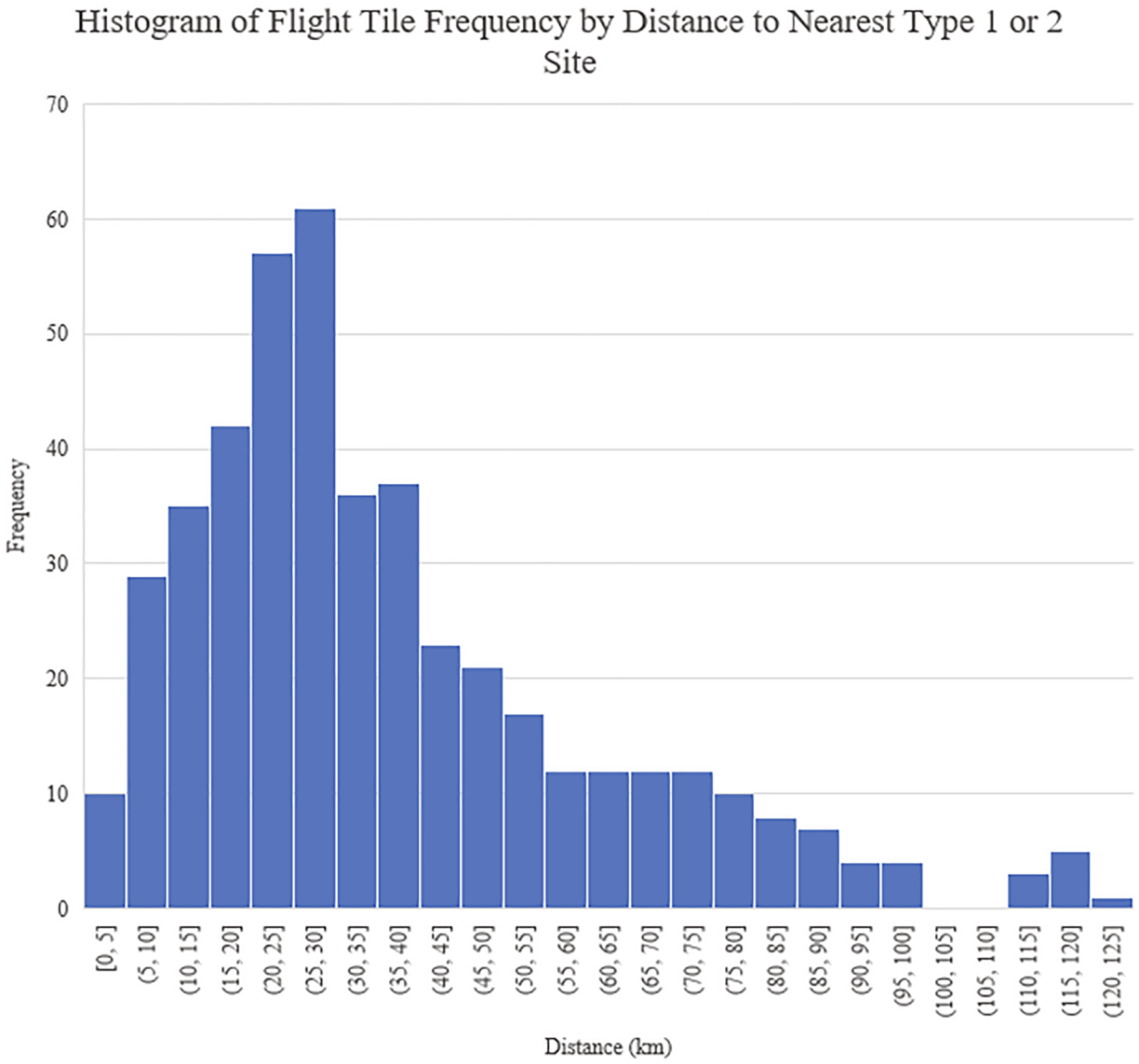

Fig. 5. Histogram of flight tile counts with distance to nearest Type 1 or 2 site (Witschey and Brown, 2010), 5 km intervals.

database, including 90% of all polygons documented. In the absence of ground verification, the counts reported in Table 1 likely underestimate the number of smaller structures, which can be difficult to visualize in areas of low vegetation; furthermore, constructed platforms versus buildings that take advantage of natural rises can be indistinguishable (Hutson et al., 2016; Magnoni et al., 2016). Agricultural terraces and walls are the most prevalent non-structure archaeological features that we documented in these data. We are continuing to study the distribution of individual features, but in this paper, we focus on structures and platforms as indices for archaeological settlement patterns and the built environment. This approach is not only consistent with recent evaluations of regional LiDAR (Canuto et al., 2018) but also the tradition of settlement pattern research across the Maya lowlands (Fedick, 1988; Ford, 1986; Murtha, 2009; Puleston, 1973; Ricketson and Ricketson, 1937). Furthermore, despite recent arguments in favor of structure footprint area and volume metrics in density calculations (Stanton et al., 2020), we relied on structure and platform counts in this first, simplified level of analysis.

5. Contextual analysis of flight paths

We revisited our original macro analysis of the ecological systems intersected by the samples described here. In this paper, we are most interested in how the distribution of archaeological features compares to what we know about the ecological systems from largescale and available GIS data. The sources of these data are listed and discussed below. We use much of the same data and retain the same three key categories based on global and national scale data discussed previously (Golden et al., 2016). The three key categories are:

Known Archaeological Context, including: *Proximity to all known sites* and *Proximity to documented 'Type 1, 2, and 3 sites'* defined by Witschey and Brown (2010).

Core Ecological Context, including: *Forested Area* provided by the Food and Agriculture Organization of the United Nations (FAO, 2012), *Soil Type and Use*, *Proximity to rivers*, *streams and water* compiled by Mexico's National Institute of Statistics and Geography (INEGI, 2000), *Rainfall and seasonality of precipitation (CoV)* downloaded from WorldClim (Fick and Hijmans, 2017, https://www.worldclim.org/) and *Physiographic region* defined by Beach and colleagues (2015, p. 2).

Modern landcover and administrative context, including: *2010 Land Use and Land Cover (250 m)* and *Protected Areas and Urbanized Areas* defined by INEGI (2010).

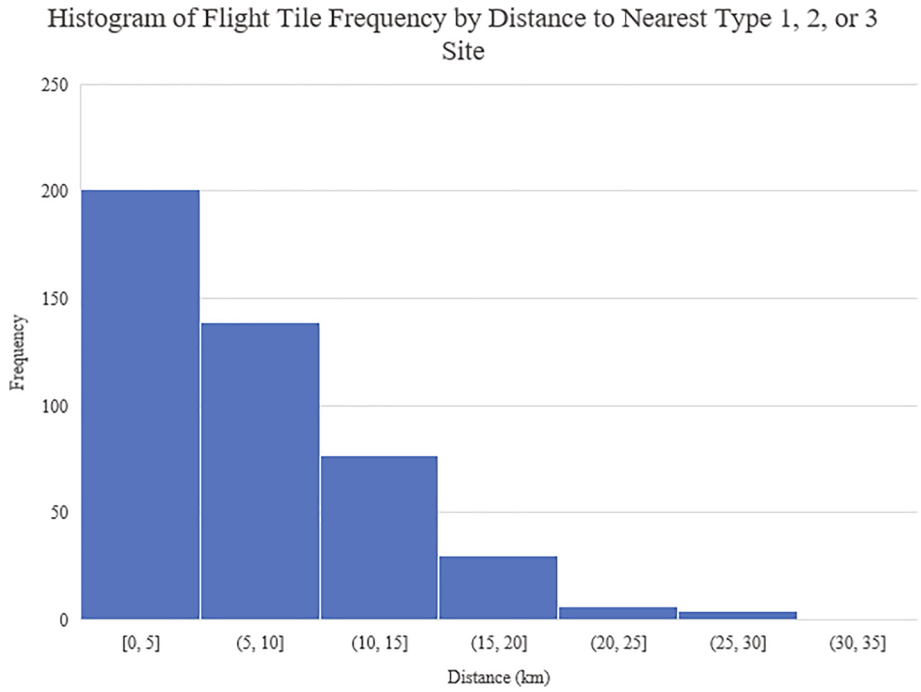

Fig. 6. Histogram of flight tile counts with distance to nearest Type 1, 2, or 3 site (Witschey and Brown, 2010), 5 km intervals.

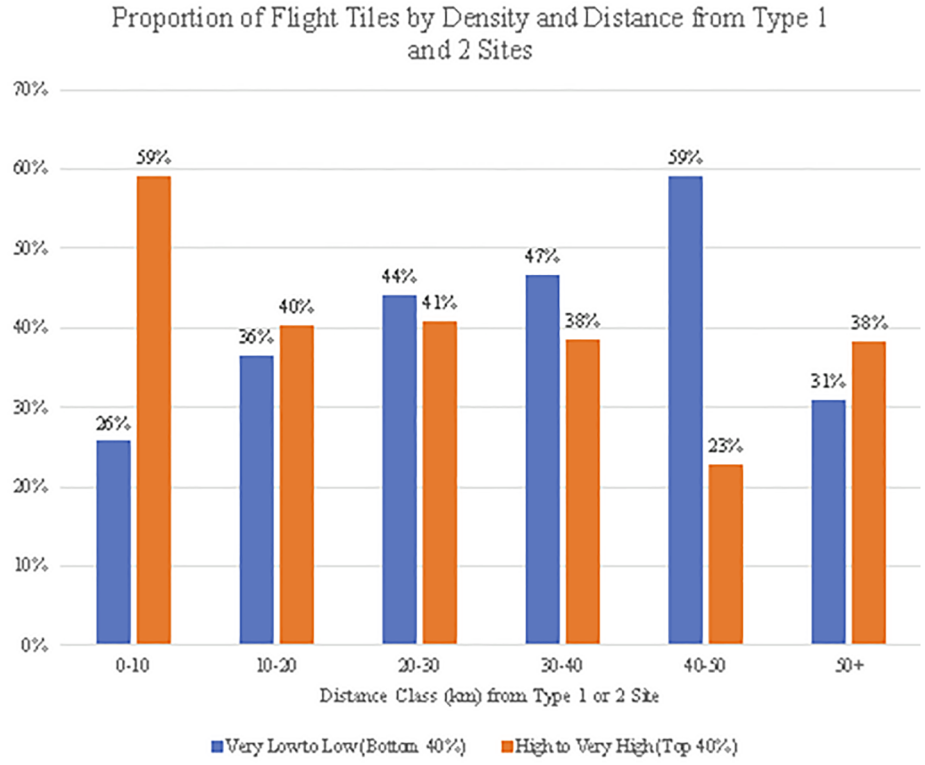

Fig. 7. Bar chart showing samples organized into 10 km distance classes with extreme structure and platform densities (bottom and top 40%) displayed as proportionally within distance classes to Type 1 and 2 sites (Witschey and Brown, 2010); middle 20% densities not shown.

Structure and platform density data based on count were classified into 5 (20%) quantile equal intervals. These intervals were ordered into density categories from very low to very high values, and the range for each category is summarized in Table 2. In the following analysis, we report relative data based on these data categories. An important conclusion from these data is the relative dispersion of structures and platforms across the sample areas. Despite areas with high densities, nearly 60% of the sample has more than 2 ha spacing per structures and platforms. These results are consistent with overall densities for the region around Tikal in the central Petén and Caracol in Western Belize, where archaeologists have observed 3–4 ha surrounding each plaza group (see Murtha, 2015).

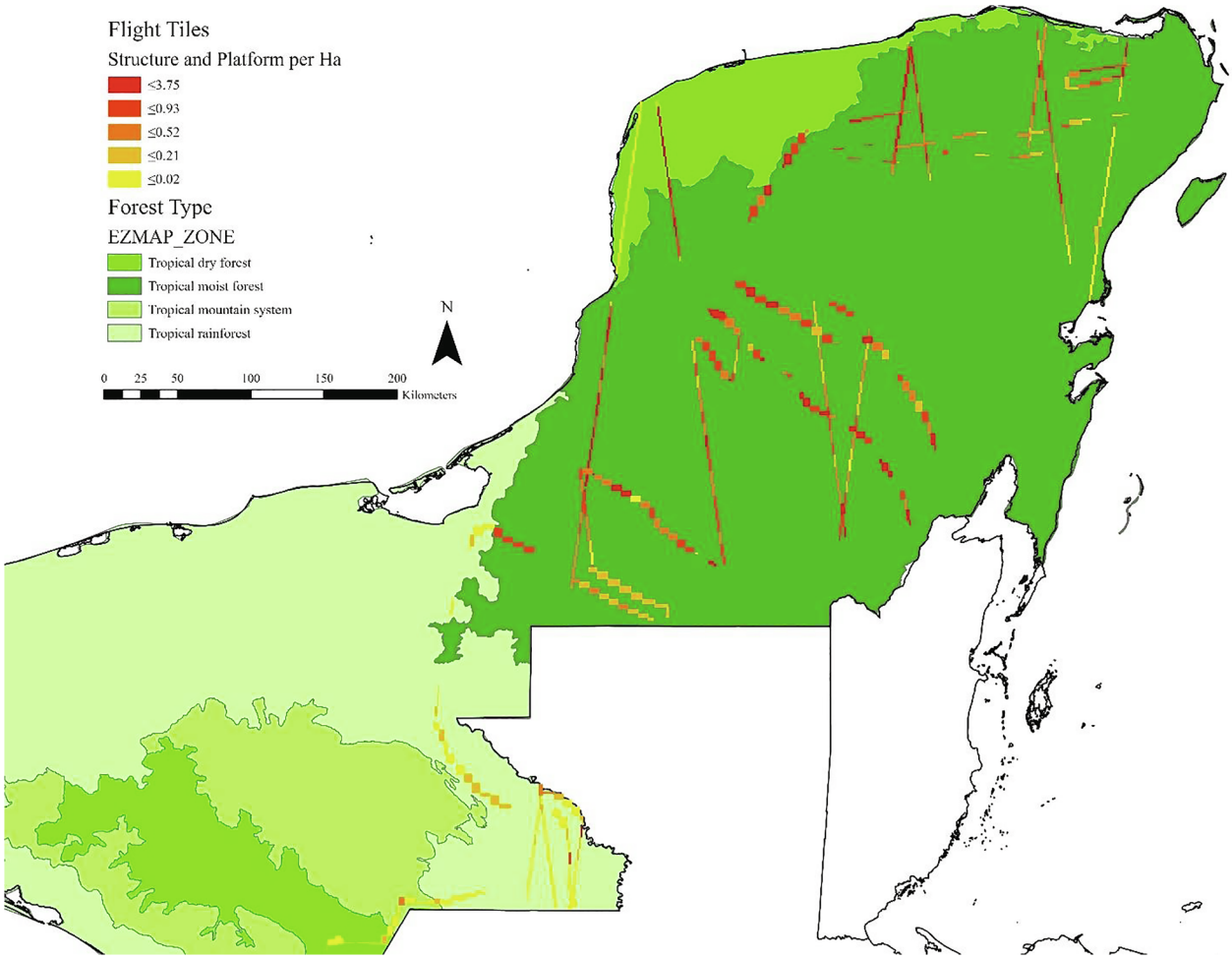

Fig. 8. Map of flight tiles and structure and platform density extrapolated to forest type (FAO, 2012).

5.1. Known archaeological context

One of the long-term goals of the current research is to compare remote sensing and curated databases of surveyed areas in the Maya lowlands. Our previous research (Golden et al., 2016) relied on the most complete and available archaeological site database for the lowlands created by Walter Witschey and Clifford Brown (2010), building off previous work (Piña Chan, 1959; Tarazona de González and Kurjack, 1980). Recognizing some inaccuracies in the spatial placement of sites in that database, and despite updates or amendments in the intervening time, to improve comparability between our two analyses, we used these data again in this paper. A more complete understanding of the relationship between flight tiles and the archaeological record will require regional collaborations with archaeological projects to include precise and accurate information from systematic survey and mapping efforts to move beyond a strict site-based approach. We hope this paper and similar approaches will serve as the first step for these collaborations. For the purposes of the initial characterization of flight tiles and archaeological features, the Witschey and Brown (2010) site data serve as a valuable proxy for archaeologically documented areas. We hope that this work and related research will catalyze efforts to expand and improve the important work by Witschey and Brown (2010).

Witschey and Brown (2010) classified the largest Maya sites based on published reports and available data into a three-tier hierarchy of settlement size following the Atlas Arqueológico del Estado de Yucatán (Tarazona de González and Kurjack, 1980). In our review of the database, Type 1 and 2 sites, while incomplete, is a representative sample of what most archaeologists would consider the largest Maya sites, and we do not distinguish between Type 1 and 2 sites. The majority of the tiles we describe here are located more than 5 km from the largest sites recorded in the Witschey and Brown (2010) database, although a plurality of flight tiles are less than 5 km away from smaller Type 3 sites (Golden et al., 2016) (Figs. 4–6). Five kilometers is used here as a catchment to reflect common patterns of site distribution and interaction across the lowlands (see Marken and Fitzsimmons, 2015). In the Northern Lowlands, the study area included samples within 5 km of Type 1 sites (e.g., Chichén Itzá, Cobá, and Izamal) and Type 2 sites (e.g., Chunchucmil, Mayapán, Xcombec, San Francisco Ticul, and San Fernando) (Arnold, 2018; Folan et al., 1983; Glover and Stanton, 2010; Hutson, 2017; Kepecs, 1998; Maler, 1997; Masson and Peraza Lope, 2014; Pollock et al., 1962). The central Campeche samples were within 5 km of the Type 2 sites Santa Rosa Xtampak and Hochob (Andrews, 1988; Morales López and Folan, 2005; de Robina, 1956). In Chiapas, no samples were within 5 km of any Type 1 or Type 2 sites. However, some samples were located within 5 km of large Type 3 sites Chinkultic and Plan de Ayutla, and another sample covered the site core of large Type 3 site Benemérito de las Américas, Primera Sección (de Borhegyi, 1968; Martos López, 2009; Mayer, 2006; Schroder et al., 2019; Tovalín and Ortiz, 2005). Two samples overlapped with sites not included in the Witschey and Brown (2010) database, including Nuevo Jalisco and El Palma, Chiapas, and El Kinel, Petén (Carrasco, 1981; Houston et al., 2006).

In all cases, structure and platform densities increase when approaching these Type 1 and 2 sites, and in the case of Chiapas, when approaching the above-mentioned large Type 3 sites. Very high densities correlate with Type 1 and 2 sites in northern Yucatán, for example

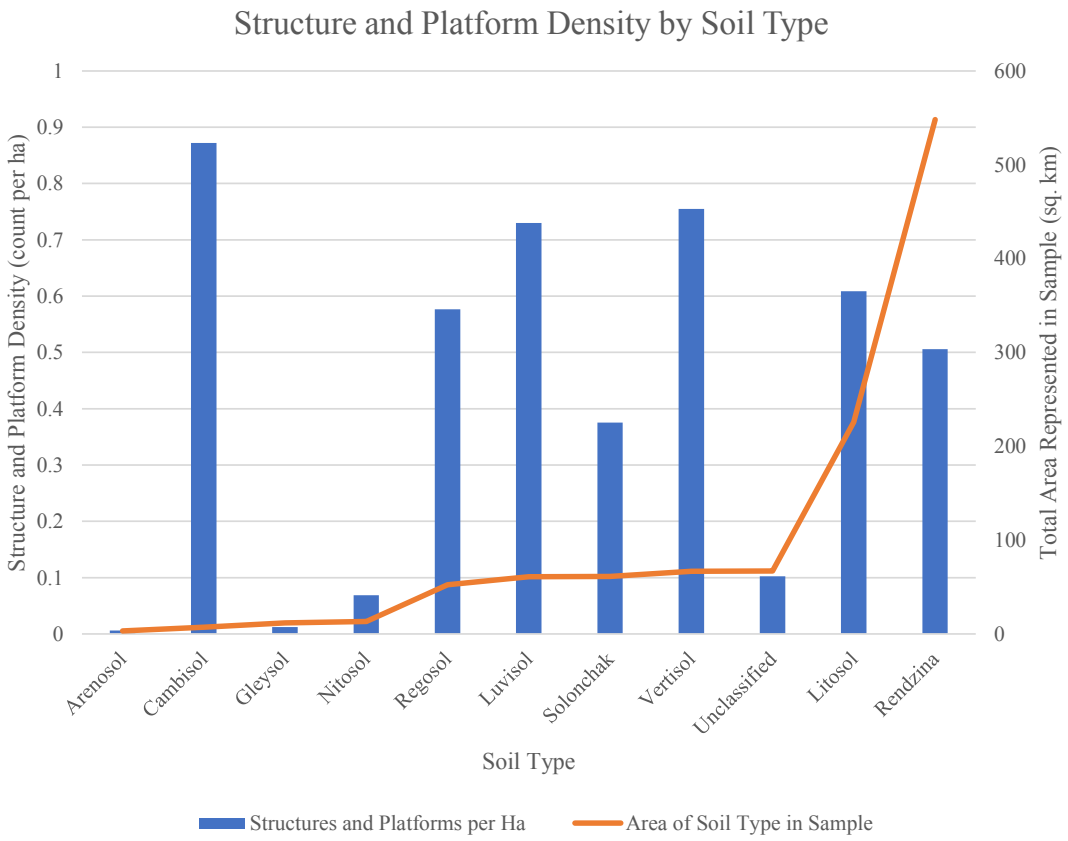

Fig. 9. Bar chart showing structure and platform density by soil type (primary, left y axis) and line chart showing the area of soil type in the sample (secondary, right y axis).

in decreasing value near Cobá, Xcombec, Chunchucmil, Izamal, Chichén Itzá, and Mayapán. The highest concentrations of Type 3 sites are also in the Northern Lowlands, and very high and high densities correlate with these locations. Densities in Chiapas are much lower in general, but densities increase closer to known sites, including high densities surrounding the Benemérito site core, medium densities near Chinkultic, the El Palma site core, and within 10 km of Yaxchilán, and low densities near Lagartero and sites in the Lacanjá River basin. These patterns persist across forested and deforested areas regardless of variations in ground point density.

Several flight samples contain high densities that do not correlate with Type 1 or 2 site locations. For example, very high densities persist 20–30 km to the north and south of Chunchucmil. These areas contain 44 Type 3 sites within a 5 km buffer. Very high densities also continue through samples within 10 km of Cobá to the north and south, and 32 Type 3 sites lie within a 5 km buffer of these flights. Furthermore, transects between Izamal and Chichén Itzá contain very high and high densities associated with 81 Type 3 sites within a 5 km buffer.

Areas in southern Campeche and southern Quintana Roo contain high to very high structure and platform densities, associated with no Type 1 or 2 sites and few if any Type 3 sites within 5 km. High densities persist for 100 km south of Campeche city, but these areas only contain 8 Type 3 sites within 5 km of the sample flight paths. Another area of interest is to the southeast of the Laguna de Términos, more than 100 km away from the nearest Type 1 or 2 site with no Type 3 sites within 5 km. This area contains a high density of features and large architecture, including monumental platforms, with no record of known sites in the Witschey and Brown (2010) database.

In summary, 59% of samples located within 10 km of a Type 1 or 2 site show very high or high densities of structures and platforms. Conversely, 38% of samples more than 10 km from a Type 1 or 2 site show very high or high densities (Fig. 7). The proportion of low and very low density tiles tends to increase as distance to known sites increases, while the proportion of high and very high density tiles remains more consistent in relation to distance. Thus, an inverse relationship between density and distance to known sites exists, but this correlation depends largely on the extent of archaeological survey and knowledge in a region. Extensive surveys in the Northern Lowlands provides abundant data to compare with the G-LiHT dataset, showing that the highest feature densities correlate with proximity to Type 1, 2, and 3 sites. However, the G-LiHT samples have also shown that high feature densities persist in areas away from the largest sites. Samples in Chiapas follow a similar pattern, with the highest feature densities occurring alongside areas with known sites. Data from central and southern Campeche underscore the importance of continued research in these regions, as they contain high feature densities but fewer documented site locations. The key conclusion from this analysis is twofold: 1) the distribution of structure and platform density is not solely related to relationship to large known archaeological site location; and, 2) it may be time for a team of archaeologists to bring together data from across the lowlands in an effort to update and refine a database similar to Witschey and Brown (2010). The G-LiHT data offer a starting point but need to be combined with more recent LiDAR efforts across the lowlands.

5.2. Core ecological context

We previously identified several macro-environmental variables to contextualize the locations of samples (FAO, 2012; Golden et al., 2016; INEGI, 2000). The environmental variables previously identified as relating to past activities, land use, and settlement include forested type, soil properties, and proximity to water, to which we have added additional variables, including annual rainfall, rainfall seasonality, and physiographic region (Beach et al., 2015; Fick and Hijmans, 2017).

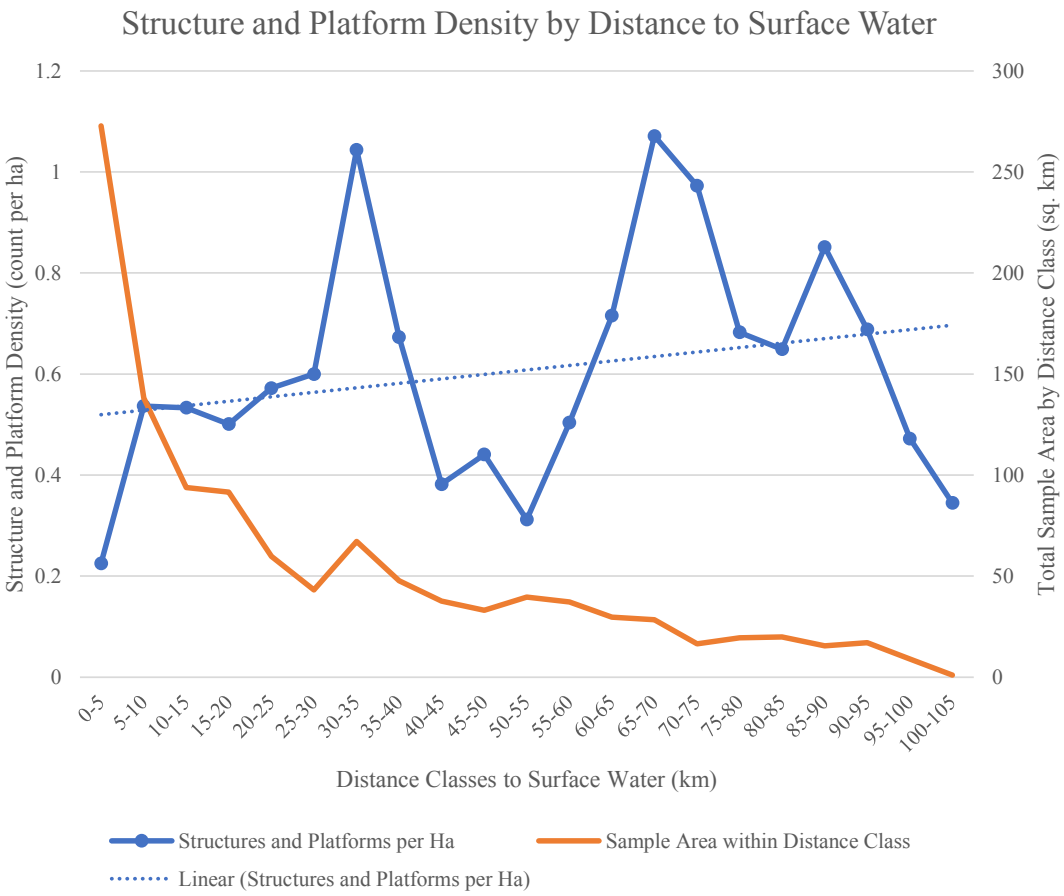

Fig. 10. Line chart showing structure and platform density by distance class from surface water (primary, left y axis) with trendline and line chart showing area of distance class within the sample (secondary, right y axis).

5.2.1. Forested type

We summarized flight path samples by forested type based on the Global EZ Level 2 – Global Ecological Zone data (FAO, 2012). Flight paths overlap with four types of forest in order of decreasing area: 1) *Tropical Moist Deciduous Forest*; 2) *Tropical Rainforest*; 3) *Tropical Dry Forest*; and 4) *Tropical Mountain System*. As observed previously, all flight paths exhibit low diversity of classified forest types, with most samples containing a single forest type, while the remainder contain no more than two types (Golden et al., 2016, p. 298).

Tropical Moist Forest and *Tropical Dry Forest* contain high densities of structures and platforms; *Tropical Rainforest* and *Tropical Mountain System* showed low densities (Fig. 8). The low density of features within *Tropical Rainforest* areas, however, is less likely due to environmental conditions and more to the location of these samples within lower density areas of the Western Maya lowlands. In fact, high densities of the built environment are known from *Tropical Rainforest* areas in other parts of the Central Lowlands (Canuto et al., 2018).

In this sample, the *Tropical Dry Forest* category contains two discrete areas, one in the northwestern Yucatan peninsula and the other in the Central Depression of Chiapas. When these two areas are treated separately, density in the northwest Yucatan (high density) is similar to other parts of the Northern Lowlands in *Tropical Moist Forests*, while *Tropical Dry Forests* in the Central Depression of Chiapas exhibit very low densities in the sample. These observations emphasize that such macro-level environmental data are insufficient in characterizing variations in settlement density; perhaps more refined local environmental data are more useful. Still, in some flight paths that cross two forest types, a notable change in structure and platform density occurs at the boundary. For example, the flight paths to the southeast of the Laguna de Términos have very low densities in *Tropical Rainforest*, but the density increases to high after crossing into areas of *Tropical Moist Forest*. This change in density is likely associated with several environmental and cultural variables influenced in part by forest type, as well as local topographic and natural drainage conditions marked by a change from low-lying wetlands to upland forest.

5.2.2. Soil properties

The sample area contains ten soil types, listed here in decreasing order of representation: rendzina, leptosol, vertisol, solonchak, luvisol, regosol, nitisol, gleysol, cambisol, and arenosol. Approximately half (50%) of the total flight sample area consisted of fine (high clay content) soils, while 42% were medium, and 2% were coarse. The majority of flight samples do not show appreciable erosion (Golden et al., 2016, p. 298).

The highest densities of structures and platforms, as well as agricultural terraces, occurred in areas of cambisol and vertisol. Cambisols generally provide productive agricultural land, but their overexploitation can lead to erosion and deterioration (Liendo Stuardo, 2002, p. 47), while vertisols are high clay content soils usually not conducive to rainfed agriculture. High structure and platform densities also occur alongside luvisols, litosols, and regosols. Unsurprisingly, very low structure and platform densities correspond with arenosol (sandy) and gleysol (wetland) soils. High-density settlements were about equally represented in fine and medium texture soils with very low densities in coarse soils (Fig. 9).

Although these data provide an initial understanding of the relationship between settlement, agriculture, and soil properties, more localized data are necessary to refine these interpretations. Furthermore, while the INEGI data provide extensive coverage, nearly 7% of the sample area's soils remain unclassified. The conclusions from

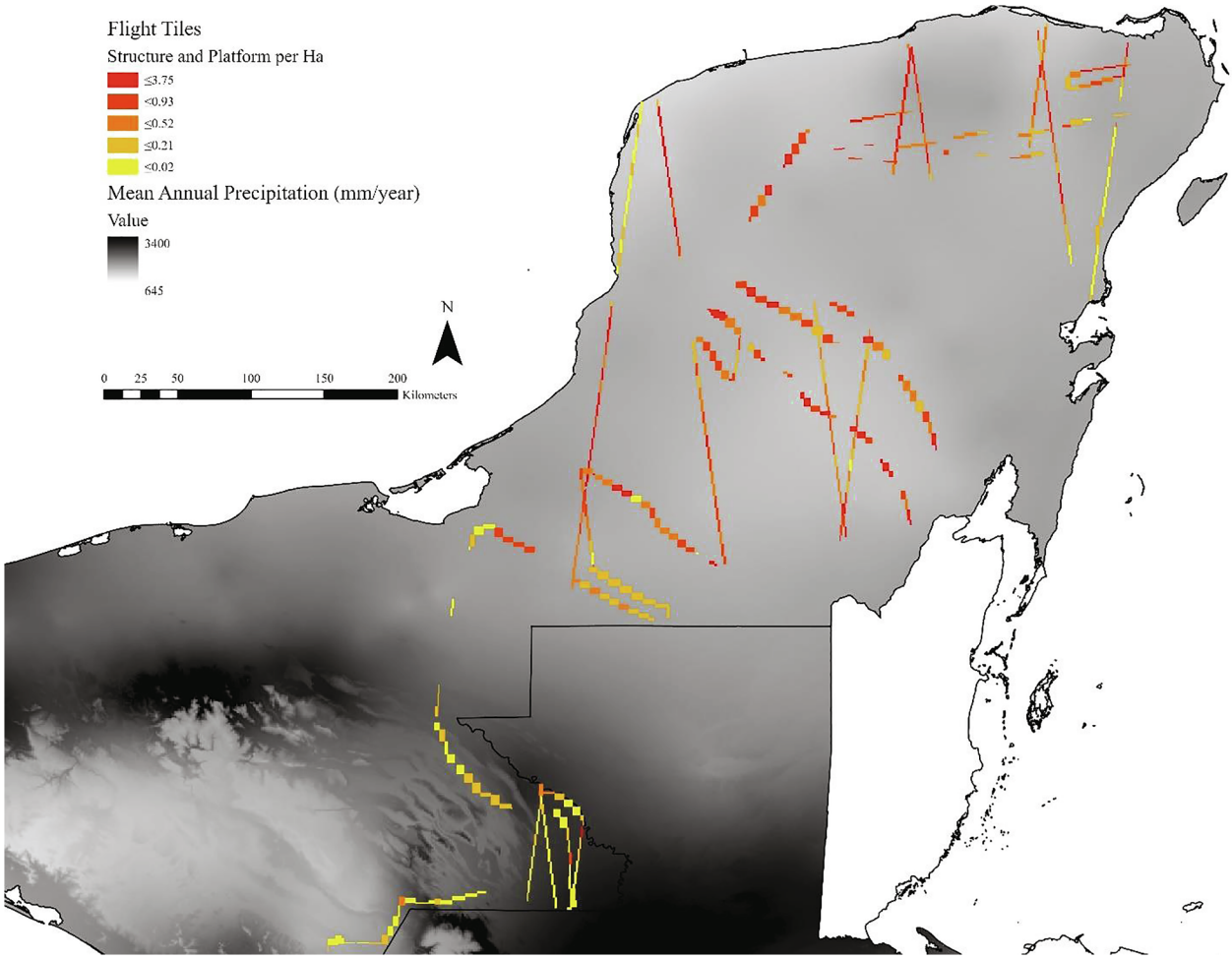

Fig. 11. Map of structure and platform density by flight tile and mean annual precipitation from WorldClim (Fick and Hijmans, 2017).

these observations are that generally speaking; soil type is a valuable predictor of Maya settlement, which is consistent with many observations about Maya settlements beginning with Sanders' (1962) speculative summary of the Cultural Ecology of the Maya lowlands (Beach et al., 2003; Dunning et al., 1994; Liendo Stuardo, 2002). We also recognize the need to develop a more complete picture of lowland soil as the next important step in our research (Bautista Zúñiga et al., 2003; Bautista Zúñiga and Palacio, 2005).

5.2.3. Proximity to surface water

INEGI 1:1,000,000 data (INEGI, 2000) provides the locations of surface water in four categories, 1) intermittent streams and rivers, 2) perennial streams and rivers, 3) intermittent lakes, and 4) perennial lakes. Surface water increases from north to southwest, with limited surface water in the Northern Lowlands and abundant streams and lakes in Chiapas. We calculated the distance from flight tile centroids to water features, finding that roughly 50% of samples are less than 20 km away from water, while the remaining samples are between 20 and 90 km from water, perennial or intermittent (Golden et al., 2016, p. 299).

The expectation is that settlement density should have an inverse relationship to distance from water, meaning that density should increase as flight samples approach surface water. However, the results of this analysis are counterintuitive; for example, average settlement densities within 0–5 km of perennial and intermittent surface water are medium, the lowest value in the distribution. This minimum value skews the data to create a direct relationship between density and distance to water, meaning that density tends to rise as distance from surface water increases (Fig. 10). Furthermore, the distribution of structure and platform density is bimodal, showing peak densities (very high) at 30–35 km and 65–70 km from all surface water. Still, the highest outlier densities are less than 30 km from surface water. Even when considering only samples from Chiapas and Tabasco, where surface water is plentiful and the farthest distance to water is 9 km (compared to 93 km in Yucatán), a weak negative correlation between distance to surface water and settlement density is present. However, in Chiapas, the highest settlement densities are within 2.5 km of water, while only low and very low densities occur above 2.5 km.

An important observation is that surface water does not take into account access to subsurface water, which is more plentiful in the form of *cenotes* and springs in some areas of high and very high-density settlements, especially in the Northern Lowlands. Moreover, some of the variations may be due to the availability of rainwater as we know the Maya were effective at managing runoff for water storage (Lucero and Fash, 2006; Scarborough, 1998, 2003; Scarborough et al., 2012b). Still, these data suggest that access to surface water was highly variable throughout the study area and was not the determining factor in settlement location.

5.2.4. Rainfall and seasonality

Rainfall and seasonality were not included in the original analysis but have been added here. Average annual precipitation and seasonality (coefficient of variation, CoV) data were downloaded from World Clim (Fick and Hijmans, 2017), and these current rainfall data were used as a proxy for past conditions in the absence of specific paleoclimatic studies (Figs. 11–12). Average annual rainfall varies from less

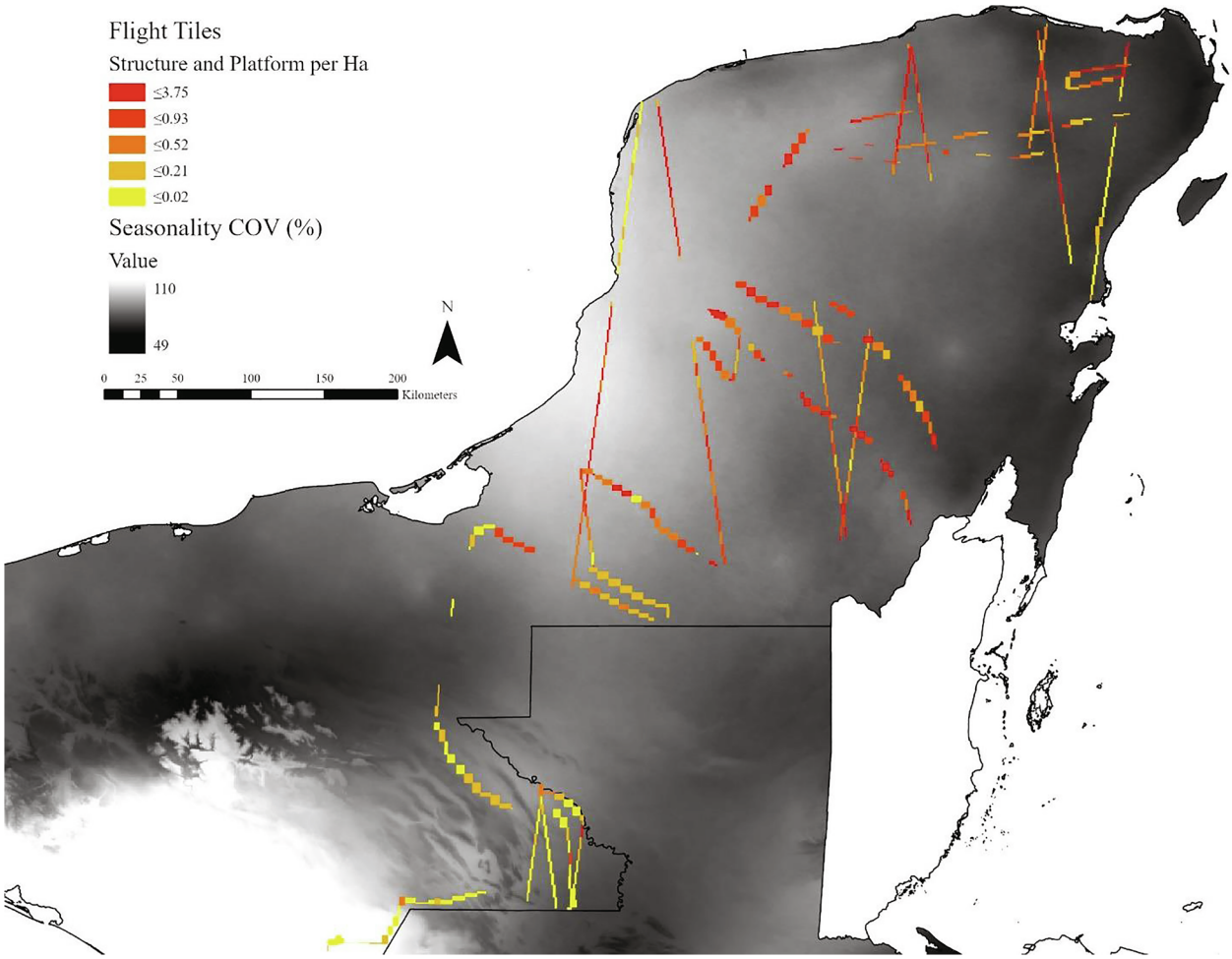

Fig. 12. Map of structure and platform density by flight tile and precipitation seasonality from WorldClim (Fick and Hijmans, 2017).

than 700 mm per year in the northwest Yucatan peninsula and generally increases to the southwest, with the highest average annual rainfall above 3300 mm per year in southeastern Chiapas. The majority of samples have annual average rainfall between 600 and 1500 mm.

WorldClim measures seasonality of precipitation as a coefficient of variation (CoV), or the ratio of the standard deviation of monthly total precipitation to the mean monthly total, reported as a percentage. The percentage can exceed 100% in instances of extreme seasonality where the standard deviation exceeds the annual mean (O'Donnell and Ignizio, 2012). Lower values reflect areas with rainfall spread evenly throughout the year, while higher values indicate increasing seasonality. All CoV values in the study area were higher than 49%, meaning that all subregions are considered to have a seasonal climate. The majority of sample areas have CoV values between 50 and 80%. In flight tiles with average rainfalls between 750 and 1200 mm, no relationship with seasonality exists. However, above 1200 mm annual rainfall, seasonality tends to decrease as rainfall increases.

Density of the built environment confirms that settlement density is highest in areas with annual rainfall between 700 and 1500 mm. Very high settlement density occurs between 700 and 900 mm of annual precipitation, with high and medium densities persisting to 1500 mm annual rainfall, while low and very low densities occur below 700 mm and above 1500 mm, respectively. Densities increase slightly in areas above 1900 mm in parts of Chiapas that correlate with larger Type 3 sites (Fig. 13). Settlement density is medium between 50 and 70% seasonality and increases to high between 70 and 90%. Above 90% seasonality, density decreases to very low (Fig. 14). Settlement density, therefore, is fairly consistent except when influenced by areas with increasingly protracted dry seasons. In contrast, agricultural terrace density shows a clear correlation with seasonality, with a linear density of terraces increasing directly with seasonality until dropping off at 90%. In summary, areas of lower annual precipitation show higher densities of settlement, while areas of higher seasonality show more evidence of agricultural intensification.

5.2.5. *Physiographic region*

To reflect the environmental and cultural diversity of the Maya area, we overlaid our analysis with a recent study of physiographic sub-regions by Beach and colleagues (Beach et al., 2015; Dunning et al., 1998; Dunning and Beach, 2010). These physiographic sub-regions classified based on local environmental, geological, and cultural conditions are expected to influence the location of archaeological features more than macro-environmental data (e.g., forest type). The G-LiHT flight tiles transect approximately half (17) of these 33 physiographic sub-regions, including from north to south (with numbers from the original in parentheses): North Coast (1); Northwest Karst Plain (3); Northeast Karst Plain (4); Yalahau (5); Puuc-Santa Elena (7); Puuc-Bolonchen Hills (8); Cobá-Okop (6); Central Hills (9); Edzna-Silvituk Trough (10); Quintana Roo Depression (11); Uayamil (12); Caribbean Reef and Eastern Coastal Margin (2); Río Candelaria-Río San Pedro (13); Petén Karst Plateau and Mirador Basin (14); Highland Ranges and Valleys (28); Río de la Pasion (20); and Chiapas, Grijalva River (32).

Structure and platform density generally decreases from north to south. The physiographic sub-regions with very high densities include the Northwest Karst Plain, Uayamil, and Puuc-Bolonchen Hills, while high densities occur in the Northeast Karst Plain, Central Hills,

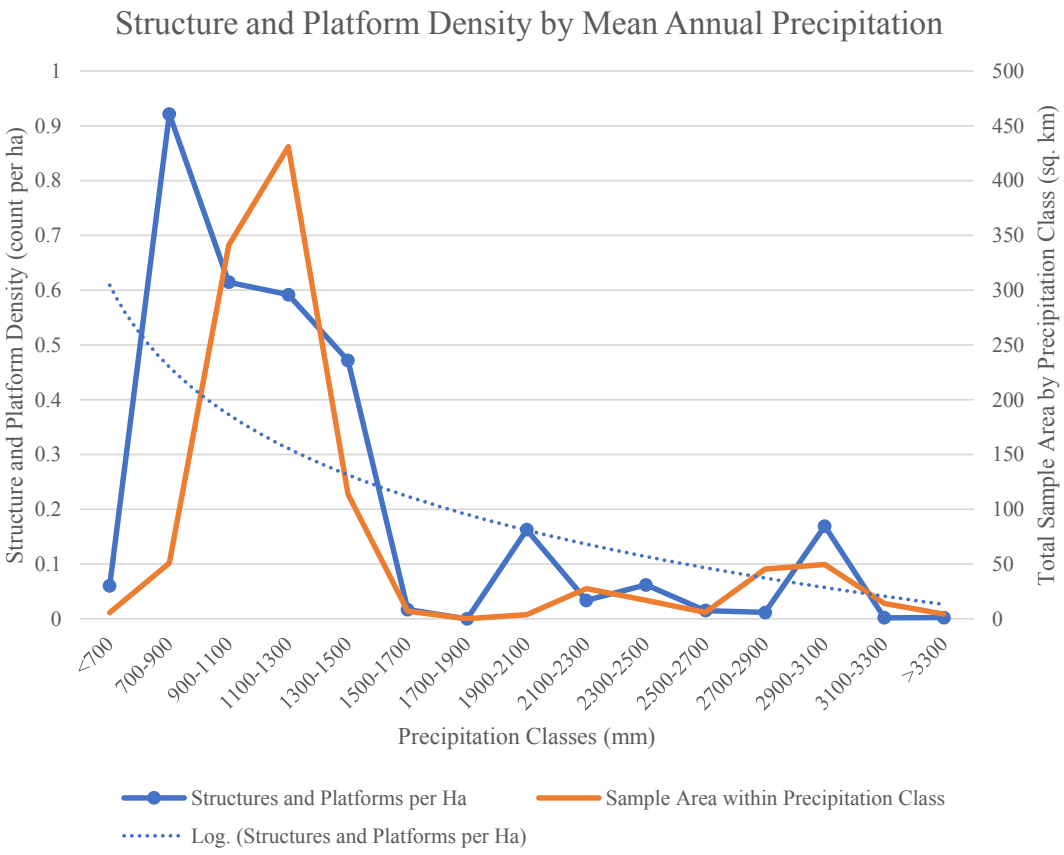

Fig. 13. Line chart showing structure and platform density by mean annual precipitation class (primary, left y axis) with logarithmic trendline and line chart showing area of precipitation class within the sample (secondary, right y axis).

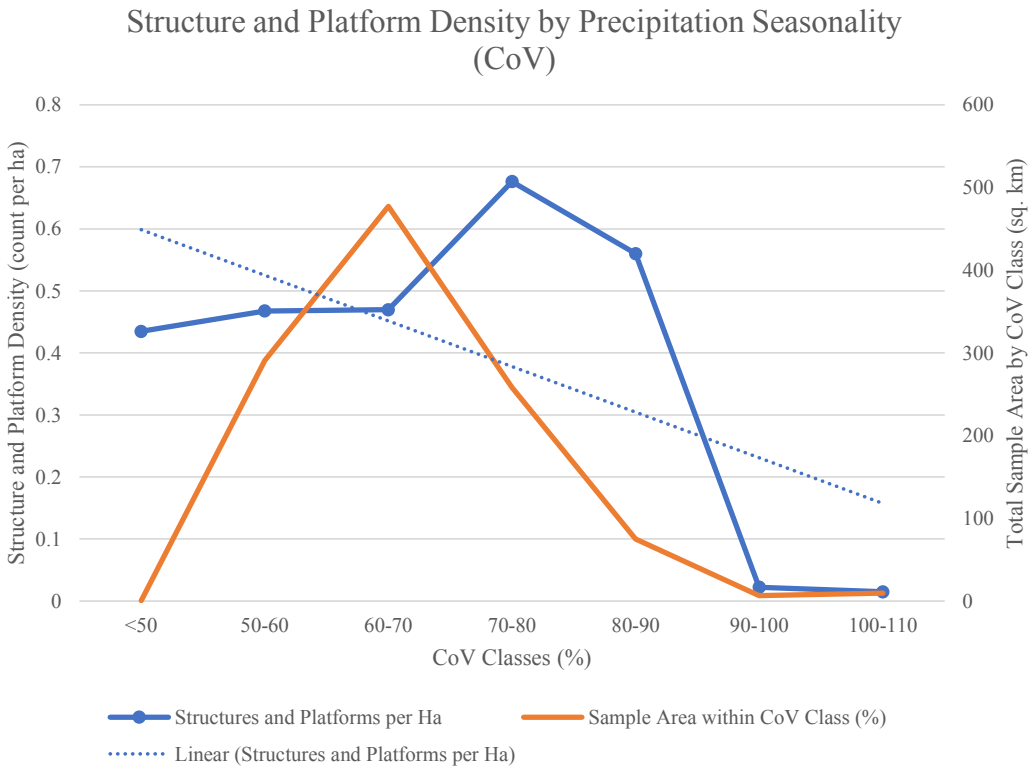

Fig. 14. Line chart showing structure and platform density by precipitation seasonality class (primary, left y axis) with trendline and line chart showing area of precipitation seasonality class within the sample (secondary, right y axis).

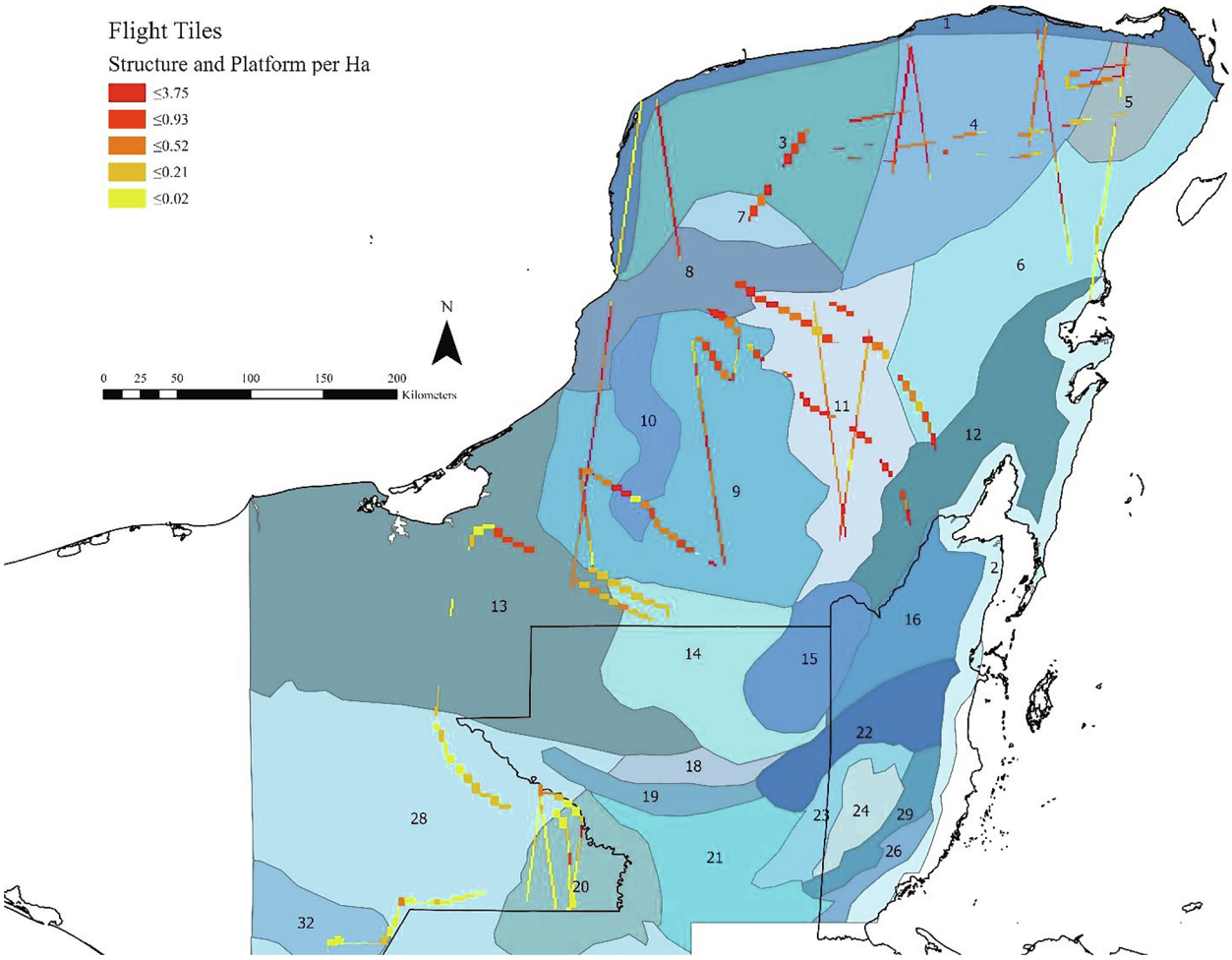

Fig. 15. Map of flight tiles and structure and platform density and physiographic sub-regions, see text for codes (Beach et al., 2015, p. 2).

Quintana Roo Depression, Yalahau, Puuc-Santa Elena, and Edzna-Silvituk Trough. Very low and low densities are found in parts of Chiapas (Chiapas, Grijalva River, and Highland Ranges and Valleys) and coastal areas (Caribbean Reef and Eastern Coastal Margin and North Coast) (Fig. 15). Agricultural terracing is most common in hilly areas of Yucatan, Campeche, and Quintana Roo states, including the Río Bec area (Quintana Roo Depression and Uayamil).

The results of this analysis show that a regional approach that incorporates physiographic and cultural data has more potential than individual site locations in predicting feature density. Still, archaeological features show marked heterogeneity across and within these physiographic subregions, and feature density is especially variable in the Río Candelaria-Río San Pedro and Cobá-Okop regions. These findings are consistent with observations from Beach and colleagues (2015, p. 5), Scott Fedick (1996), and other researchers that the Maya region is not monolithic and is instead environmentally diverse between, within, and beyond its traditionally defined lowland and highland areas.

5.3. Modern landcover and administrative context

Modern land use and landcover are relevant to the processing and quality of data analyzed in the G-LiHT samples, as well as characterizing threats to the preservation of cultural resources. Land use variables, however, are constantly changing, presenting challenges to an analysis of contemporary landcover. Land use data compiled by INEGI (2010) provide the most appropriate dataset to approximate land use conditions during the 2013 GLiHT study. Furthermore, we relate the results of our analysis with the proximity to protected and urban areas, assessing conservation threats to cultural resources.

5.3.1. 2010 Land use and land cover

The INEGI (2010) land use data contain numerous nested categories. To simplify the current analysis, data were dissolved into nine unique categories and four mixed categories: 1) agricultural area (including irrigated and seasonal), 2) urban area, 3) area with no vegetation, 4) forest (temperate montane forest, gallery forest, oak and pine forest, and oak forest), 5) body of water (perennial maritime and perennial interior), 6) other types of vegetation (popal, savannah, and mangrove), 7) foreign country (Guatemala), 8) pasture (including cultivated and induced grassland), 9) jungle (high, evergreen canopy; low, deciduous canopy; low, semi-deciduous canopy; and medium, semi-deciduous canopy), 10) agricultural area-pasture, 11) agricultural area-jungle, 12) other types of vegetation-pasture, and 13) pasture-jungle. The data also contain relevant information related to the presence of secondary forest and appreciable erosion. The majority of flight tiles cover areas defined as jungle, amounting to approximately 70% of the total surveyed area. The next largest categories are pasture and jungle-pasture, each representing less than 10% of the total area of samples.

Very high densities of structures and platforms are located in areas of mixed agriculture and jungle with consistently high densities throughout areas of jungle, pasture, and agriculture or mixtures of these categories. Very low densities lie in urban areas, forests, and areas without vegetation. The lowest densities of archaeological features in urban areas and areas without vegetation point to the threats of

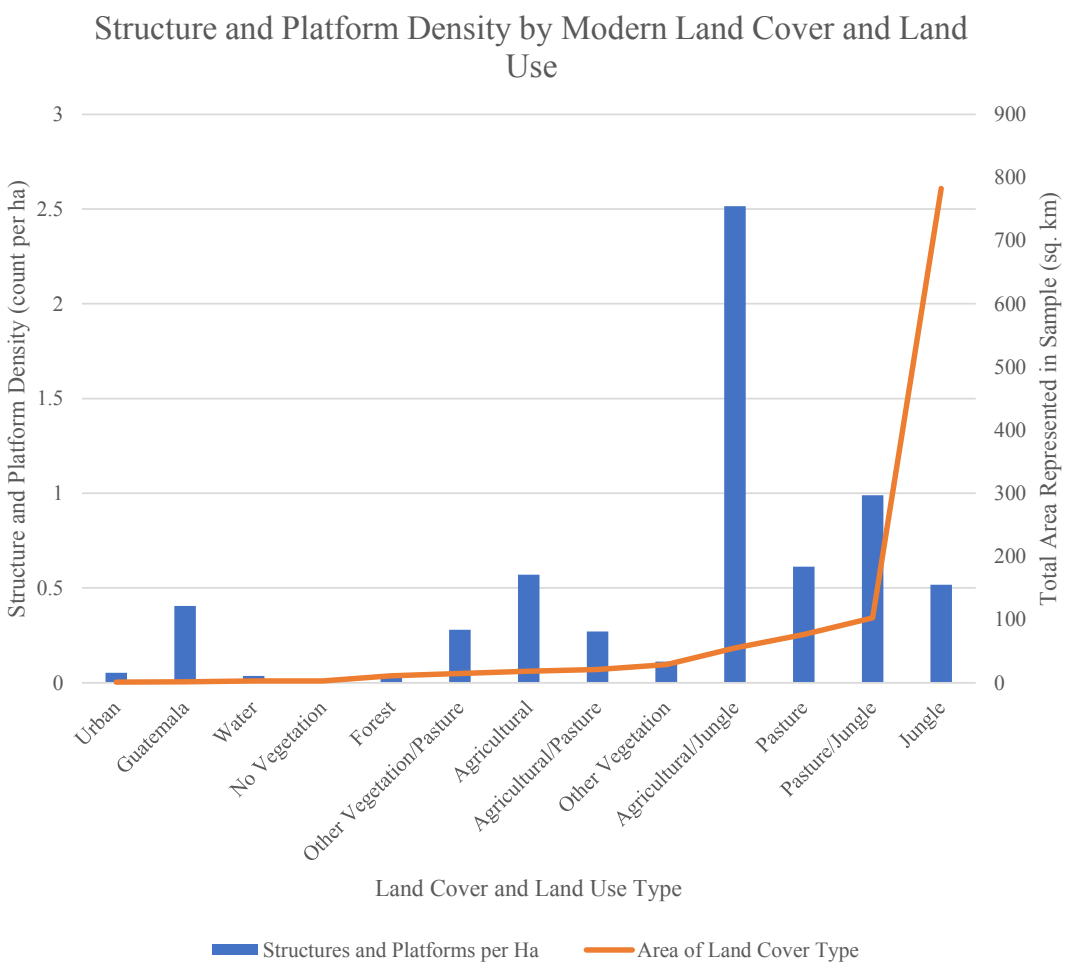

Fig. 16. Bar chart showing structure and platform density by land cover type (primary, left y axis) and line chart showing area of land cover type in the sample (secondary, right y axis).

deforestation on cultural resources, while the relatively low densities in forest and jungle environments compared to agricultural areas and pastureland suggests some level of processing issues in certain types of evergreen vegetation (Fig. 16).

5.3.2. Protected areas and urbanized areas

Flight samples cross several protected areas, including in decreasing order of representation Montes Azules Biosphere Reserve (12), Bala'an K'aax Protected Area (8), Los Petenes Biosphere Reserve (3), Lacan-Tun Biosphere Reserve (14), Calakmul Biosphere Reserve (11), Ría Celestún Biosphere Reserve (2), Balam-Kú Reserve (10), Sian Ka'an Biosphere Reserve (7), El Palmar Conservation Zone (1), Balam-Kin Reserve (9), Chan-Kin Reserve (15), Lagunas de Montebello Biosphere Reserve (16), Bonampak (13), Ría Lagartos Biosphere Reserve (4), Yum Balam Protection Area (5), and the Arrecifes de Sian Kaan Biosphere Reserve (6) (Fig. 17). In total, the proportion of protected areas amounts to 17.6% of the combined sample area.

The density of structures and platforms demonstrates that four protected areas contain high values, including Calakmul, Balam-Kin, El Palmar, and Balam-Kú. Although adjacent to El Palmar, the Petenes and Ría Celestún areas show a marked decrease to a very low built environment density. The overall density of features within protected areas is low to medium compared to the high density of features outside of protected areas.

Most flight tiles avoided urban areas, with a plurality of samples collected within 30 and 40 km of urban areas (Golden et al. 2016). Only four tiles intersect directly with the limits of two urban areas (defined as any population center over 2,000 individuals), Cenotillo and Valladolid, Yucatán. As expected, no archaeological features were documented in areas that intersected with urban zones. However, structure and platform density near these urban areas is highly variable, ranging from low within 5 km of Valladolid to very high within 5 km of Cenotillo.

Structure and platform density were relatively consistent across distance classes; however, high-density areas include those closest and furthest from urban areas, in decreasing order within distance classes of 100–110 km, 20–30 km, 0–10 km, and 50–60 km (Fig. 18). The remaining distance classes all contain a medium density of features. The high density of structures and platforms within 10 km of urban areas, and the very high density within 5 km of Cenotillo, underscores that much of the archaeological record (9% of all features documented in this analysis, compared to 4% of all features in protected areas) is threatened by urban development.

6. Summary and conclusions

In this analysis, we have confirmed the value and potential of an extensive LiDAR survey in opening the doors to new and complementary anthropological questions when comparing past settlement patterns and density to modern environmental, land use, and conservation variables, especially in the context of transformative surveys conducted in other regions of the lowlands. The G-LiHT data present a balance of well-studied areas and under-documented portions of the landscape to fill in gaps in understanding while building on regional expertise and knowledge developed from decades of research. The possibilities for collaboration are promising to develop models that

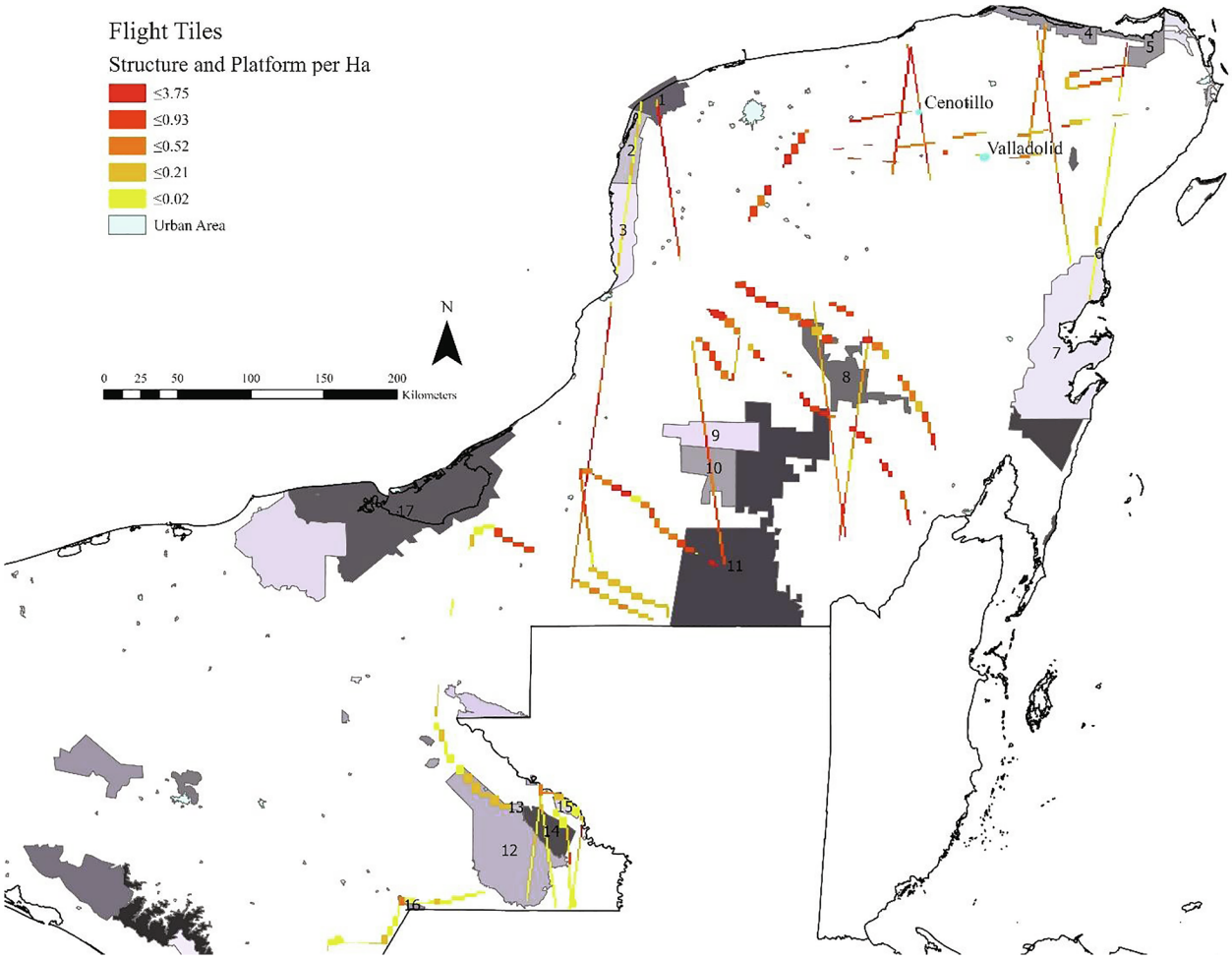

Fig. 17. Map of flight tiles, urban areas (with urban areas overlapping tiles highlighted and labeled), and structure and platform density extrapolated to protected areas in Mexico, codes represent protected areas within the study area and the Laguna de Términos (17), mentioned in the text, see text for codes (CONANP, 2020).

center landscape and environmental studies away from traditional site-based approaches. This study has also sought to advance LiDAR and remote sensing technologies away from their use as a tool for site prospection toward a form of analysis that can develop important research questions or approach old frameworks from new perspectives.

Structure and platform densities annotated over 458 samples over southern Mexico have identified relationships between the built environment and several environmental, cultural, and archaeological variables. Of these contextual analyses, known archaeological sites, forest type, soil properties, access to surface water, rainfall and seasonality, and previously defined physiographic regions affected settlement density and agricultural intensification to various degrees. We conclude that among the variables analyzed, known archaeological site location, physiographic region, and modern precipitation patterns are the strongest predictors for feature density. Still, rather than highlighting clear patterns, these data show high diversity across subregions not defined by any single variable. Instead, the effects on settlement density were influenced by a combination of environmental, cultural, and historical variables; some presented here and others undoubtedly omitted and to be included in future research. Our study focused on settlement density, as defined by structure and platform count, while further research will analyze the distribution of specific feature types.

An important finding from this analysis is that in areas of prior archaeological research, these data follow previously established patterns, showing consistency of results across approaches in remote sensing and pedestrian survey. For instance, high settlement densities in the Northern Lowlands match the abundant data compiled from archaeological surveys in this region, likely due to a long history of landscape use and reuse from the Preclassic through the Colonial periods. The data from Chiapas confirm observations made by archaeologists over decades of survey in the region that overall settlement densities tend to be lower than those observed in Yucatán, while larger populations and political centers often cluster near resources, such as arable land, bodies of water, defensive locations, or access to trade routes (Aliphat Fernández, 1994; Anaya Hernández, 2001; Golden et al., 2012; Scherer and Golden, 2009; Schroder et al., 2017).

The structure densities from this analysis, especially those from the Central Lowlands, are consistent with—and are in fact higher than—recent LiDAR surveys in Guatemala (Canuto et al., 2018), which estimate an aggregate settlement density of 29 structures per square kilometer in contrast to 49 structures per square kilometer in our annotations. These results are especially significant due to the distinct sampling strategies used in each study, the former focusing primarily on large political centers and the latter on the wider settlement and agrarian landscape. We report here, however, only the results of initial analysis, with the caveats that these data require ground verification and further analysis to interpret chronology and function. What these initial results offer is an opportunity to quantify relative differences in settlement density and to assess to what extent distinct but related environmental and cultural variables affected the observed diversity. These data also demonstrate that despite unexpected densities across the lowlands, agricultural land is generally abundant. Understanding

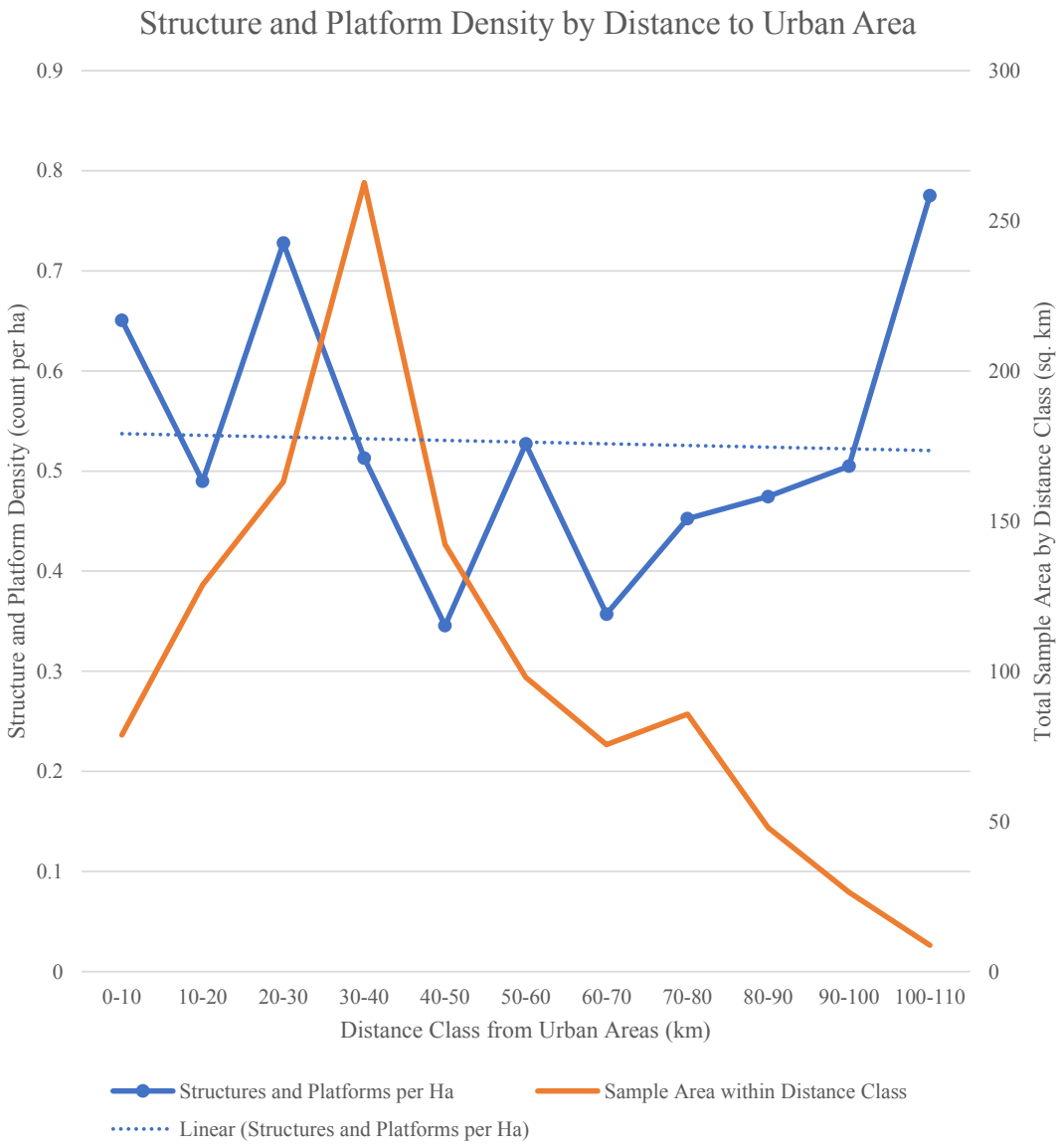

Fig. 18. Line chart showing structure and platform density by distance class to urban areas (primary, left y axis) with trendline and line chart showing the area of distance class within the sample (secondary, right y axis).

the variance in the distribution of these agrarian landscapes is an important next step of our research.

Finally, we encourage further collaboration among archaeologists, environmental scientists, and policymakers based on the results of this analysis. We have a unique opportunity emerging to link our discrete observations into larger open datasets to accommodate more robust and complete spatial analysis of features and how they compare to archaeological chronologies and the location of specific resources. Contextual analyses of environmental data will benefit from more localized, intensive research rather than the reliance on extensive, macroecological variables we have adopted. Furthermore, the analysis of land use from data collected in 2010 highlights the benefit of LiDAR not merely in documenting archaeological resources but rather on tracking changes in modern land use over time. These shifts in modern landcover, protected areas, and urban zones present threats to the archaeological and environmental records, and conservation efforts are best focused on developing strategies that mitigate such challenges together. We expect our ongoing research to contribute to these goals by addressing themes of landscape resilience and sustainability in historical and contemporary Maya land use.

CRediT authorship contribution statement

Whittaker Schroder: Data curation, Writing - original draft, Conceptualization, Methodology, Formal analysis, Visualization. **Timothy Murtha:** Data curation, Writing - original draft, Conceptualization, Methodology, Visualization, Verification. **Charles Golden:** Conceptualization, Writing - review & editing. **Armando Anaya Hernández:** Conceptualization, Writing - review & editing. **Andrew Scherer:** Conceptualization, Writing - review & editing. **Shanti Morell-Hart:** Conceptualization, Writing - review & editing. **Angélica Almeyda Zambrano:** Conceptualization, Writing - review & editing. **Eben Broadbent:** Conceptualization, Writing - review & editing. **Madeline Brown:** Conceptualization, Writing - review & editing, Verification.

Acknowledgments

Funding in support of this research was provided by the National Science Foundation (BCS#1849921) and the National Aeronautics and Space Administration (19-IDS19-0060). Lidar data were collected by

Dr. Hank Margolis (NASA Headquarters, ProgramManager, NASA Terrestrial Ecology Program) with support from a NASA Carbon Cycle Science award to Ross Nelson (Program Announcement Number NNH10ZDA001N-CARBON). We also thank the reviewers for their comments on an earlier version of this manuscript. Field research in Mexico is supported by the Instituto Nacional de Antropología e Historia.

References

Abrams, E.M., 1994. How the Maya built their world: energetics and ancient architecture. University of Texas Press, Austin.

Ainsworth, S., Oswald, A., Went, D., 2013. Remotely acquired, not remotely sensed: using lidar as a field survey tool. In: Opitz, R.S., Cowley, D.C. (Eds.), Interpreting Archaeological Topography: Airborne Laser Scanning, 3D Data and Ground Observation, Occasional Publication of the Aerial Archaeology Research Group. Oxbow Books, Oxford, pp. 206–222.

Alexander, R.T., 1999. Mesoamerican house lots and archaeological site structure: problems of inference in Yaxcaba, Yucatan, Mexico, 1750–1847. In: Allison, P.M. (Ed.), The Archaeology of Household Activities. Routledge, Abingdon, pp. 78–100.

Aliphat Fernández, M.M., 1994. Classic Maya landscape in the Upper Usumacinta river valley (Unpublished. PhD dissertation). University of Calgary.

Anaya Hernández, A., 2001. Site interaction and political geography in the Upper Usumacinta region during the Late Classic: a GIS approach, BAR International Series 994. J. and E, Hedges, Oxford.

Andrews, G.F., 1988. Architectural survey: Santa Rosa Xtampak. University of Oregon, Eugene.

Arnauld, M.C., Michelet, D., Nondédéo, 2013. Living together in Río Bec houses: coresidence, rank, and alliance. Ancient Mesoamerica 24, 469–493. https://doi.org/10.1017/S0956536114000029.

Arnold, D.E., 2018. Maya potters' indigenous knowledge: cognition, engagement, and practice. University Press of Colorado, Boulder.

Arnott, S., Maki, D.L., 2019. Forts on Burial Mounds: Interlocked Landscapes of Mourning and Colonialism at the Dakota-Settler Frontier, 1860–1876. Hist Arch 53, 153–169. https://doi.org/10.1007/s41636-019-00169-9.

Ashmore, W., 2007. Settlement archaeology at Quiriguá. University of Pennsylvania Museum of Archaeology and Anthropology, Philadelphia, Guatemala.

Ashmore, W., 1984. Quiriguá archaeology and history revisited. J. Field Archaeol. 11, 365–386. https://doi.org/10.2307/529316.

Ashmore, W., 1981. Lowland Maya settlement patterns. School of American Research, Albuquerque.

Balkansky, A.K., Kowalewski, S.A., Pérez Rodríguez, V., Pluckhahn, T.J., Smith, C.A., Stiver, L.R., Beliaev, D., Chamblee, J.F., Heredia Espinoza, V.Y., Santos Pérez, R., 2000. Archaeological survey in the Mixteca Alta of Oaxaca, Mexico. Journal of Field Archaeology 27, 365–389. https://doi.org/10.1179/jfa.2000.27.4.365.

Banaszek, Ł., 2020. It takes all kinds of trees to make a forest. Using historic maps and forestry data to inform airborne laser scanning based archaeological prospection in woodland. Archaeological Prospection arp.1780. doi: 10.1002/arp.1780.

Barbour, T.E., Sassaman, K.E., Almeyda Zambrano, A., Broadbent, E.N., Wilkinson, B., Kanaski, R., 2019. Rare pre-Columbian settlement on the Florida Gulf Coast revealed through high-resolution drone LiDAR. PNAS 116, 23493–23498. https://doi.org/10.1073/pnas.1911285116.

Barnes, I., 2003. Aerial remote-sensing techniques used in the management of archaeological monuments on the British Army's Salisbury Plain Training Area, Wiltshire, UK. Archaeol. Prospect. 10, 83–90. https://doi.org/10.1002/arp.197.

Bautista Zúñiga, F., Batllori-Sampedro, E., Ortiz-Pérez, M.A., Palacio-Aponte, G., Castillo-González, M., 2003. Geoformas, agua y suelo de la península de Yucatán. In: Colunga-García Marín, P., Larqué-Saavedra, A. (Eds.), Naturaleza y Sociedad En El Área Maya. Academia Mexicana de Ciencias-CICY, Mérida, pp. 21–36.

Bautista Zúñiga, F., Palacio, A.G. (Eds.), 2005. Caracterización y manejo de los suelos de la peninsula de Yucatán: implicaciones agropecuarias, forestales y ambientales. Universidad Autónoma de Campeche, Campeche.

Beach, T., Dunning, N.P., Luzzadder-Beach, S., Cook, D., Lohse, J., 2006. Ancient Maya impacts on soil erosion. Catena 66, 166–178.

Beach, T., Dunning, N.P., Luzzadder-Beach, S., Scarborough, V.L., 2003. Depression soils in the lowland tropics of northwestern Belize: anthropogenic and natural origins. In: Gómez-Pompa, A., Allen, M., Fedick, S.L. (Eds.), Lowland Maya Area: Three Millenia at the Human-Wildland Interface. Haworth Press, Binghamton, NY.

Beach, T., Luzzadder-Beach, S., Cook, D., Dunning, N., Kennett, D.J., Krause, S., Terry, R., Trein, D., Valdez, F., 2015. Ancient Maya impacts on the Earth's surface: an early Anthropocene analog? Quat. Sci. Rev. 124, 1–30. https://doi.org/10.1016/j.quascirev.2015.05.028.

Beach, T., Luzzadder-Beach, S., Dunning, N.P., 2008. Human and natural impacts on fluvial and karst depressions of the Maya lowlands. Geomorphology 101 (1/2), 301–331.

Beach, T., Luzzadder-Beach, S., Dunning, N.P., Jones, J.G., Lohse, J., Guderjan, T., Bozarth, S., Millspaugh, S., Bhattachary, T., 2009. A review of human and natural changes in Maya lowland wetlands over the Holocene. Quat. Res. 28, 1710–1724.

Beach, T., Luzzadder-Beach, S., Krause, S., Guderjan, T., Valdez, F., Fernández-Diaz, J.C., Eshleman, S., Doyle, C., 2019. Ancient Maya wetland fields revealed under tropical forest canopy from laser scanning and multiproxy evidence. Proc Natl Acad Sci USA 201910553. https://doi.org/10.1073/pnas.1910553116.

Beach, T.P., Luzzadder-Beach, S., Dunning, N.P., Terry, R., Houston, S., Garrison, T., 2011. Carbon isotopic ratios of wetland and terrace soil sequences in the Maya lowlands of Belize and Guatemala. Catena 85, 109–118.

Becker, M.J., 1982. Ancient Maya houses and their identification: an evaluation of architectural groups at Tikal and inferences regarding their functions. Revista Española de Antropología Americana 12, 111–129.

Bedford, S., Siméoni, P., Lebot, V., 2018. The anthropogenic transformation of an island landscape: Evidence for agricultural development revealed by LiDAR on the island of Efate, Central Vanuatu, South-West Pacific. Archaeology in Oceania 53, 1–14. https://doi.org/10.1002/arco.5137.

Beex, W.F., 2017. Lessons from LiDAR data use in the Netherlands. 1 1, 661–670.

Benjamin, J., O'Leary, M., Ward, I., Hacker, J., Ulm, S., Veth, P., Holst, M., McDonald, J., Ross, P.J., Bailey, G., 2018. Underwater archaeology and submerged landscapes in western Australia. Antiquity 92, e10. https://doi.org/10.15184/aqy.2018.103.

Bernardini, F., Sgambati, A., Montagnari Kokelj, M., Zaccaria, C., Micheli, R., Fragiacomo, A., Tiussi, C., Dreossi, D., Tuniz, C., De Min, A., 2013. Airborne LiDAR application to karstic areas: the example of Trieste province (north-eastern Italy) from prehistoric sites to Roman forts. J. Archaeol. Sci. 40, 2152–2160.

Bewley, R., Crutchley, S., Shell, C., 2005. New light on an ancient landscape: lidar survey in the Stonehenge World Heritage Site. Antiquity 79, 636–647.

Brewer, J.L., Carr, C., Dunning, N.P., Walker, D.S., Anaya Hernández, A., Peuramaki-Brown, M., Reese-Taylor, K., 2017. Employing airborne lidar and archaeological testing to determine the role of small depressions in water management at the ancient Maya site of Yaxnohcah, Campeche, Mexico. J. Archaeolog. Sci.: Rep. 13, 291–302. https://doi.org/10.1016/j.jasrep.2017.03.044.

Bullard Jr., W.R., 1952. Residential property walls at Mayapán. In: Current Reports. Carnegie Institution of Washington, Washington, DC, pp. 36–44.

Cain, T.C., 2019. Materializing political violence: segregation, war, and memory in Quintana Roo, Mexico (Unpublished PhD dissertation). University of Pennsylvania, Philadelphia.

Canuto, M., Estrada-Belli, F., Garrison, T.G., Houston, S.D., Acuña, M.J., Kováč, M., Marken, D., Nondédéo, P., Auld-Thomas, L., Castanet, C., Chatelain, D., Chiriboga, C.R., Drápela, T., Lieskovský, T., Tokovinine, A., Velasquez, A., Fernández-Díaz, J.C., Shrestha, R., 2018. Ancient lowland Maya complexity as revealed by airborne laser scanning of northern Guatemala. Science 361. https://doi.org/10.1126/science.aau0137.

Carrasco, R., 1981. Informe del sitio arqueológico Nuevo Jalisco, Chis., in: de la Garza, M. (Ed.), Estudios de Cultura Maya, Vol. XIII. Centro de Estudios Mayas, UNAM, Mexico City.

Carson, J.F., Whitney, B.S., Mayle, F.E., Iriarte, J., Prümers, H., Soto, J.D., Watling, J., 2014. Environmental impact of geometric earthwork construction in pre-Columbian Amazonia. PNAS 111, 10497–10502.

Chase, A.F., Chase, D.Z., 2017. Detection of Maya Ruins by LiDAR: Applications, Case Study, and Issues. In: Masini, N., Soldovieri, F. (Eds.), Sensing the Past: From Artifact to Historical Site. Springer, Cham, Switzerland, pp. 455–468. https://doi.org/10.1007/978-3-319-50518-3_22.

Chase, A.F., Chase, D.Z., Awe, J.J., Weishampel, J.F., Iannone, G., Moyes, H., Yaeger, J., Brown, M.K., 2014a. The use of LiDAR in understanding the ancient Maya landscape: Caracol and western Belize. Adv. Archaeol. Pract.: A J. Soc. Am. Archaeol. 2, 208–221. https://doi.org/10.7183/2326-3768.2.3.208.

Chase, A.F., Chase, D.Z., Awe, J.J., Weishampel, J.F., Iannone, G., Moyes, H., Yaeger, J., Brown, M.K., Shrestha, R., Carter, W.E., Fernández-Díaz, J.C., 2014b. Ancient Maya regional settlement and inter-site analysis: the 2013 west-central Belize LiDAR survey. Remote Sens. 6, 8671–8695.

Chase, A.F., Chase, D.Z., Fisher, C.T., Leisz, S.J., Weishampel, J.F., 2012. Geospatial revolution and remote sensing LiDAR in Mesoamerican archaeology. Proc. Natl. Acad. Sci. 109, 12916–12921. https://doi.org/10.1073/pnas.1205198109.

Chase, A.F., Chase, D.Z., Weishampel, J.F., 2010. Lasers in the Jungle. Archaeology 28.

Chase, A.F., Chase, D.Z., Weishampel, J.F., Drake, J.B., Shrestha, R.L., Slatton, K.C., Awe, J.J., Carter, W.E., 2011. Airborne LiDAR, archaeology, and the ancient Maya landscape at Caracol, Belize. J. Archaeol. Sci. 38, 387–398.

Chevance, J.-B., Evans, D., Hofer, N., Sakhoeun, S., Chhean, R., 2019. Mahendraparvata: an early Angkor-period capital defined through airborne laser scanning at Phnom Kulen. Antiquity 93, 1303–1321. https://doi.org/10.15184/aqy.2019.133.

Chiba, T., Kaneta, S., Suzuki, Y., 2008. Red relief image map: new visualization method for three dimensional data. The International Archives of the Photogrammetry, Remote Sensing and Spatial Information Sciences 37, 1071–1076.

Comer, D.C., Comer, J.A., Dumitru, I.A., Ayres, W.S., Levin, M.J., Seikel, K.A., White, D.A., Harrower, M.J., 2019. Airborne LiDAR Reveals a Vast Archaeological Landscape at the Nan Madol World Heritage Site. Remote Sens. 11, 2152. https://doi.org/10.3390/rs11182152.

CONANP, 2020. Áreas naturales protegidas de México [WWW Document]. URL http://sig.conanp.gob.mx/website/interactivo/anps/.

Cook, B., Corp, L., Nelson, R., Middleton, E., Morton, D., McCorkel, J., Masek, J., Ranson, K., Ly, V., Montesano, P., 2013. NASA Goddard's LIDAR, hyperspectral and thermal (G-LiHT) airborne imager. Remote Sens. 5, 4045–4066.

Davis, D.S., Lipo, C.P., Sanger, M.C., 2019a. A comparison of automated object extraction methods for mound and shell-ring identification in coastal South Carolina. J. Archaeolog. Sci.: Rep. 23, 166–177. https://doi.org/10.1016/j.jasrep.2018.10.035.

Davis, D.S., Sanger, M.C., Lipo, C.P., 2019b. Automated mound detection using lidar and object-based image analysis in Beaufort County, South Carolina. Southeastern Archaeology 38, 23–37. https://doi.org/10.1080/0734578X.2018.1482186.

de Borhegyi, S.F., 1968. Archaeological reconnaissance of the Chinkultic, Chiapas, Mexico, Publication 26.6. Middle American Research Institute, New Orleans.

de Matos Machado, R., Hupy, J.P., 2019. The Conflict Landscape of Verdun, France: Conserving Cultural and Natural Heritage After WWI. In: Lookingbill, T.R., Smallwood, P.D. (Eds.), Collateral Values. Springer International Publishing, Cham,

pp. 111–132. https://doi.org/10.1007/978-3-030-18991-4_5.
De Reu, J., Bourgeois, J., Bats, M., Zwertvaegher, A., Gelorini, V., De Smedt, P., Chu, W., Antrop, M., De Maeyer, P., Finke, P., Van Meirvenne, M., Verniers, J., Crombé, P., 2013. Application of the topographic position index to heterogeneous landscapes. Geomorphology 186. https://doi.org/10.1016/j.geomorph.2012.12.015.
Demarest, A.A., O'Mansky, M., Wolley, C., Van Turenhout, D., Inomata, T., Palka, J., Escobedo, H.L., 1997. Classic Maya defensive systems and warfare in the Petexbatun region. Ancient Mesoamerica 8, 229–253. https://doi.org/10.1017/S095653610000170X.
Doneus, M., Briese, C., Fera, M., Janner, M., 2008. Archaeological prospection of forested areas using full-waveform airborne laser scanning. J. Archaeol. Sci. 35, 882–893. https://doi.org/10.1016/j.jas.2007.06.013.
Donkin, R.A., 1979. Agricultural terracing in the aboriginal New World. University of Arizona Press, Tucson.
Dunning, J.B., Danielson, B.J., Pulliam, H.R., 1992. Ecological processes that affect populations in complex landscapes. Oikos 65, 169–175. https://doi.org/10.2307/3544901.
Dunning, N., 1997. The paleoecology and ancient settlement of the Petexbatun region, Guatemala. Ancient Mesoamerica 8, 255–266.
Dunning, N., Scarborough, V.L., Valdez, F., Luzzadder-Beach, S., Beach, T., Jones, J.G., 1999. Temple mountains, sacred lakes, and fertile fields: ancient Maya landscapes in northwestern Belize. Antiquity 73, 650–660.
Dunning, N.P., 1996. A reexamination of regional variability in the prehistoric agricultural landscape. In: Fedick, S.L. (Ed.), The Managed Mosaic: Ancient Maya Agriculture and Resource Use. University of Utah Press, Salt Lake City, pp. 53–68.
Dunning, N.P., Anaya Hernández, A., Beach, T., Carr, C., Griffin, R., Jones, J.G., Lentz, D.L., Luzzadder-Beach, S., Reese-Taylor, K., Šprajc, I., 2019. Margin for error: anthropogenic geomorphology of bajo edges in the Maya lowlands. Geomorphology 331, 127–145. https://doi.org/10.1016/j.geomorph.2018.09.002.
Dunning, N.P., Beach, T., 2004. Noxious or nurturing nature? Maya civilization in environmental context. In: Golden, C.W., Borgstede, G. (Eds.), Continuities and Changes in Maya Archaeology. Routledge Press, New York.
Dunning, N.P., Beach, T., Rue, D.J., 1994. Soil erosion, slope management, and ancient terracing in the Maya lowlands. Latin American Antiquity 5, 51–69.
Dunning, N.P., Beach, T.P., 2010. Farms and forests: spatial and temporal perspectives on ancient Maya landscapes. In: Martini, I.P., Chesworth, W. (Eds.), Landscapes and Societies. Springer, New York, pp. 369–389.
Dunning, N.P., Luzzadder-Beach, S., Beach, T., Jones, J.G., Scarborough, V.L., Culbert, T.P., 2002. Arising from the bajos: the evolution of a neotropical landscape and the rise of Maya civilization. Ann. Assoc. Am. Geogr. 92, 267–283.
Dunning, N.P., Rue, D.J., Beach, T., Covich, A., Traverse, A., 1998. Human-environmental interactions in a tropical watershed: the paleoecology of Laguna Tamarandito, El Petén, Guatemala. Journal of Field Archaeology 25, 139–151. https://doi.org/10.1179/009346998792005487.
Ebert, C.E., Hoggarth, J.A., Awe, J.J., 2016. Integrating Quantitative Lidar Analysis and Settlement Survey in the Belize River Valley. Adv. archaeol. pract. 4, 284–300. https://doi.org/10.7183/2326-3768.4.3.284.
Evans, D., Fletcher, R., 2015. The landscape of Angkor Wat redefined. Antiquity 89, 1402–1419. https://doi.org/10.15184/aqy.2015.157.
Falconer, S.E., Savage, S.H., 1995. Heartlands and hinterlands: alternative trajectories of early urbanization in Mesopotamia and the southern Levant. Am. Antiq. 60, 37–58. https://doi.org/10.2307/282075.
FAO, 2012. Global ecological zones for FAO forest reporting: 2010 update. Forest Resources Assessment Working Paper 179, Rome, 2012.
Fedick, S.L., 1996. Introduction: new perspectives on ancient Maya agriculture and resource use. In: Fedick, S.L. (Ed.), The Managed Mosaic: Ancient Maya Agriculture and Resource Use. University of Utah Press, Salt Lake City, pp. 1–14.
Fedick, S.L., 1994. Ancient Maya agricultural terracing in the Upper Belize River area: computer-aided modeling and the results of initial field investigations. Ancient Mesoamerica 5, 107–127.
Fedick, S.L., 1988. Prehistoric Maya settlement and land use patterns in the upper Belize River area, Belize, Central America (Unpublished PhD dissertation). Arizona State University, Tempe.
Fedick, S.L., Ford, A., 1990. The prehistoric agricultural landscape of the Central Maya Lowlands: an examination of local variability in a regional context. World Archaeology 22, 18–33.
Fernández-Diaz, J., Carter, W., Shrestha, R., Glennie, C., 2014. Now You See It… Now You Don't: Understanding Airborne Mapping LiDAR Collection and Data Product Generation for Archaeological Research in Mesoamerica. Remote Sens. 6, 9951–10001. https://doi.org/10.3390/rs6109951.
Fernández-Diaz, J.C., 2019. Flights into the past: archaeological prospection using Lidar. LIDAR Magazine Webinar Series, 23 October 2019. https://www.youtube.com/watch?v=v8PiAGSVpJQ (accessed 7 October 2020).
Fernández-Diaz, J.C., Cohen, A.S., 2020. Whose Data Is It Anyway? Lessons in Data Management and Sharing from Resurrecting and Repurposing Lidar Data for Archaeology Research in Honduras. J. Comput. Appl. Archaeol. 3, 122–134. https://doi.org/10.5334/jcaa.51.
Fick, S.E., Hijmans, R.J., 2017. WorldClim 2: new 1km spatial resolution climate surfaces for global land areas. Int. J. Climatol. 37, 4302–4315. https://doi.org/10.1002/joc.5086.
Fisher, C.T., Cohen, A.S., Fernández-Diaz, J.C., Leisz, S.J., 2017. The application of airborne mapping LiDAR for the documentation of ancient cities and regions in tropical regions. Quat. Int. 448, 129–138. https://doi.org/10.1016/j.quaint.2016.08.050.
Fisher, C.T., Fernández-Diaz, J.C., Cohen, A.S., Neil Cruz, O., Gonzáles, A.M., Leisz, S.J., Pezzutti, F., Shrestha, R., Carter, W., 2016. Identifying Ancient Settlement Patterns through LiDAR in the Mosquitia Region of Honduras. PLoS ONE 11, e0159890. https://doi.org/10.1371/journal.pone.0159890.
Fisher, C.T., Leisz, S.J., 2013. New Perspectives on Purépecha Urbanism Through the Use of LiDAR at the Site of Angamuco, Mexico. Mapping Archaeological Landscapes from Space. Springer 199–210.
Fisher, C.T., Leisz, S.J., Outlaw, G., 2011. Lidar - A valuable tool uncovers an ancient city in Mexico 77, 962–967.
Folan, W.J., Kintz, E.R., Fletcher, L.A., 1983. Coba: a Classic Maya metropolis. Academic Press, New York.
Ford, A., 1986. Population growth and social complexity: an examination of settlement and environment in the central Maya lowlands. Arizona State University, Tempe, Anthropological Research Papers.
Garrison, T.G., 2010. Remote sensing ancient Maya rural populations using QuickBird satellite imagery. Int. J. Remote Sens. 31, 213–231. https://doi.org/10.1080/01431160902882629.
Garrison, T.G., Chapman, B., Houston, S., Román, E., Garrido López, J.L., 2011. Discovering ancient Maya settlements using airborne radar elevation data. J. Archaeol. Sci. 38, 1655–1662. https://doi.org/10.1016/j.jas.2011.02.031.
Garrison, T.G., Houston, S.D., Golden, C., Inomata, T., Nelson, Z., Munson, J., 2008. Evaluating the use of IKONOS satellite imagery in lowland Maya settlement archaeology. J. Archaeol. Sci. 35, 2770–2777. https://doi.org/10.1016/j.jas.2008.05.003.
George-Chacón, S.P., Dupuy, J.M., Peduzzi, A., Hernández-Stefanoni, J.L., 2019. Combining high resolution satellite imagery and lidar data to model woody species diversity of tropical dry forests. Ecol. Ind. 101, 975–984.
Glover, J.B., Stanton, T.W., 2010. Assessing the role of Preclassic traditions in the formation of Early Classic Yucatec cultures, México. J. Field Archaeol. 35, 58–77. https://doi.org/10.1179/009346910X12707320296711.
Golden, C., Murtha, T., Cook, B., Shaffer, D.S., Schroder, W., Hermitt, E.J., Alcover Firpi, O., Scherer, A.K., 2016. Reanalyzing environmental lidar data for archaeology: Mesoamerican applications and implications. J. Archaeolog. Sci.: Rep. 9, 293–308. https://doi.org/10.1016/j.jasrep.2016.07.029.
Golden, C., Scherer, A., Muñoz, A.R., Hruby, Z., 2012. Polities, boundaries, and trade in the Classic period Usumacinta river basin. Mexicon 34, 11–19.
Gómez-Pompa, A., Allen, M.F., Fedick, S.L., Jiménez-Osornio, J.J. (Eds.), 2003. Lowland Maya area: three millennia at the human-wildland interface. Haworth Press, Binghamton, NY.
Hare, T., Masson, M., Russell, B., 2014. High-Density LiDAR Mapping of the Ancient City of Mayapán. Remote Sens. 6, 9064–9085. https://doi.org/10.3390/rs6099064.
Hare, T.S., Masson, M.A., 2012. Intermediate-scale patterns in the urban environment of Postclassic Mayapán. In: The Neighborhood as a Social and Spatial Unit in Mesoamerican Cities. The University of Arizona Press, Tucson, pp. 229–260.
Henry, E.R., Shields, C.R., Kidder, T.R., 2019. Mapping the Adena-Hopewell Landscape in the Middle Ohio Valley, USA: Multi-Scalar Approaches to LiDAR-Derived Imagery from Central Kentucky. J Archaeol Method Theory. https://doi.org/10.1007/s10816-019-09420-2.
Hernández-Stefanoni, J.L., Dupuy, J.M., Johnson, K., Birdsey, R., Tun-Dzul, F., Peduzzi, A., Caamal-Sosa, J.P., Sánchez-Santos, G., López-Merlín, D., 2014. Improving species diversity and biomass estimates of tropical dry forests using airborne LiDAR. Remote Sens. 6, 4741–4763.
Hernández-Stefanoni, J.L., Johnson, K.D., Cook, B.D., Dupuy, J.M., Birdsey, R., Peduzzi, A., Tun-Dzul, F., 2015. Estimating species richness and biomass of tropical dry forests using LIDAR during leaf-on and leaf-off canopy conditions. Appl. Veg. Sci. 18, 724–732.
Hernández-Stefanoni, J.L., Reyes-Palomeque, G., Castillo-Santiago, M.Á., George-Chacón, S.P., Huechacona-Ruiz, A.H., Tun-Dzul, F., Rondon-Rivera, D., Dupuy, J.M., 2018. Effects of sample plot size and GPS location errors on aboveground biomass estimates from LiDAR in tropical dry forests. Remote Sens. 10, 1586.
Hightower, J., Butterfield, A., Weishampel, J., 2014. Quantifying Ancient Maya Land Use Legacy Effects on Contemporary Rainforest Canopy Structure. Remote Sens. 6, 10716–10732. https://doi.org/10.3390/rs61110716.
Horn, S.W., Ford, A., 2019. Beyond the magic wand: methodological developments and results from integrated Lidar survey at the ancient Maya Center El Pilar. Science & Technology of Archaeological Research, STAR, pp. 1–15.
Houston, S.D., Escobedo, H.L., Golden, C., Scherer, A., Vásquez, R., Arroyave, A.L., Quiroa, F., Meléndez, J.C., 2006. La Técnica and El Kinel: mounds and monuments upriver from Yaxchilán. Mexicon 28, 87–93.
Hutson, S.R., 2017. Ancient Maya commerce. University Press of Colorado, Boulder.
Hutson, S.R., 2015. Adapting LiDAR data for regional variation in the tropics: A case study from the Northern Maya Lowlands. J. Archaeolog. Sci.: Rep. 4, 252–263. https://doi.org/10.1016/j.jasrep.2015.09.012.
Hutson, S.R., Kidder, B., Lamb, C., Vallejo-Cáliz, D., Welch, J., 2016. Small Buildings and Small Budgets: Making Lidar Work in Northern Yucatan. Mexico. Adv. archaeol. pract. 4, 268–283. https://doi.org/10.7183/2326-3768.4.3.268.
Hutson, S.R., Magnoni, A., Mazeau, D., Stanton, T.W., 2006. The archaeology of urban houselots at Chunchucmil, Yucatan, Mexico. In: Mathews, J., Morrison, B. (Eds.), Lifeways in the Northern Lowlands: New Approaches to Maya Archaeology. University of Arizona Press, Tucson, pp. 77–92.
Hutson, S.R., Stanton, T.W., Magnoni, A., Terry, R., Craner, J., 2007. Beyond the buildings: formation processes of ancient Maya houselots and methods for the study of non-architectural space. J. Anthropol. Archaeol. 26, 442–473. https://doi.org/10.1016/j.jaa.2006.12.001.
INEGI, 2010. Uso de suelo y vegetación [WWW Document]. URL https://www.inegi.org.mx/temas/usosuelo/.
INEGI, 2000. Carta hidrología [WWW Document]. URL https://www.inegi.org.mx/temas/hidrologia/.
Inomata, T., Pinzón, F., Ranchos, J.L., Haraguchi, T., Nasu, H., Fernández-Diaz, J.C.,

Aoyama, K., Yonenobu, H., 2017. Archaeological Application of Airborne LiDAR with Object-Based Vegetation Classification and Visualization Techniques at the Lowland Maya Site of Ceibal, Guatemala. Remote Sens. 9, 563. https://doi.org/10.3390/rs9060563.
Inomata, T., Triadan, D., Aoyama, K., Castillo, V., Yonenobu, H., 2013. Early ceremonial constructions at Ceibal, Guatemala, and the origins of the lowland Maya civilization. Science 340, 467–471.
Inomata, T., Triadan, D., Pinzón, F., Aoyama, K., 2019. Artificial plateau construction during the Preclassic period at the Maya site of Ceibal, Guatemala. PLoS ONE 14, e0221943. https://doi.org/10.1371/journal.pone.0221943.
Inomata, T., Triadan, D., Pinzón, F., Burham, M., Ranchos, J.L., Aoyama, K., Haraguchi, T., 2018. Archaeological application of airborne LiDAR to examine social changes in the Ceibal region of the Maya lowlands. PLoS ONE 13, e0191619. https://doi.org/10.1371/journal.pone.0191619.
Inomata, T., Triadan, D., Vázquez López, V.A., Fernández-Diaz, J.C., Omori, T., Méndez Bauer, M.B., García Hernández, M., Beach, T., Cagnato, C., Aoyama, K., Nasu, H., 2020. Monumental architecture at Aguada Fénix and the rise of Maya civilization. Nature. https://doi.org/10.1038/s41586-020-2343-4.
Johnson, K.M., Ouimet, W.B., 2014. Rediscovering the lost archaeological landscape of southern New England using airborne light detection and ranging (LiDAR). J. Archaeol. Sci. 43, 9–20.
Jones, B.D., Bickler, S.H., 2017. High Resolution LiDAR data for Landscape Archaeology in New Zealand. Archaeology in New Zealand 60, 35–44.
Kepecs, S., 1998. Diachronic ceramic evidence and its social implications in the Chikinchel region, northeast Yucatan, Mexico. Ancient Mesoamerica 9, 121–135. https://doi.org/10.1017/S0956536100001899.
Kincey, M., Challis, K., 2010. Monitoring fragile upland landscapes: The application of airborne lidar. J. Nat. Conserv. 18, 126–134. https://doi.org/10.1016/j.jnc.2009.06.003.
Kincey, M., Challis, K., Howard, A.J., 2008. Modelling selected implications of potential future climate change on the archaeological resource of river catchments: an application of geographical information systems. Conserv. Manag. Archaeol. Sites 10, 113–131. https://doi.org/10.1179/175355209X435560.
Kintz, E.R., 1983. Neighborhoods and wards in a Classic Maya metropolis. In: Folan, W.J., Kintz, E.R., Fletcher, L.A. (Eds.), Coba: A Classic Maya Metropolis. Academic Press, New York, pp. 179–190.
Kokalj, Ž., Somrak, M., 2019. Why Not a Single Image? Combining Visualizations to Facilitate Fieldwork and On-Screen Mapping. Remote Sens. 11, 747. https://doi.org/10.3390/rs11070747.
Kokalj, Ž., Zakšek, K., Oštir, K., 2011. Application of sky-view factor for the visualisation of historic landscape features in lidar-derived relief models. Antiquity 85, 263–273.
Kokalj, Ž., Zakšek, K., Oštir, K., 2010. Archaeological Application of an Advanced Visualisation Technique Based on Diffuse Illumination, in: Proceedings of the 30th EARSeL Symposium: Remote Sensing for Science, Education Natural and Cultural Heritage. pp. 113–9.
Kolb, M.J., Snead, J.E., 1997. It's a small world after all: comparative analyses of community organization in archaeology. Am. Antiq. 62, 609–628. https://doi.org/10.2307/281881.
Kowalewski, S.A., 1990. The evolution of complexity in the Valley of Oaxaca. Annual Review of Anthropology 19, 39–58. https://doi.org/10.1146/annurev.an.19.100190.000351.
LeCount, L.J., Walker, C.P., Blitz, J.H., Nelson, T.C., 2019. Land tenure systems at the ancient Maya site of Actuncan, Belize. Latin American Antiquity 30, 245–265. https://doi.org/10.1017/laq.2019.16.
Lemonnier, E., Vannière, B., 2013. Agrarian features, farmsteads, and homesteads in the Río Bec nuclear zone. Mexico 24, 397–413. https://doi.org/10.1017/S0956536113000242.
Liebmann, M.J., Farella, J., Roos, C.I., Stack, A., Martini, S., Swetnam, T.W., 2016. Native American depopulation, reforestation, and fire regimes in the Southwest United States, 1492–1900 CE. PNAS 113, E696–E704. https://doi.org/10.1073/pnas.1521744113.
Liendo Stuardo, R., 2002. The organization of agricultural production at a Maya center: settlement patterns in the Palenque region, Chiapas, México. Serie Arqueología de México. Instituto Nacional de Antropología e Historia and University of Pittsburgh. Mexico City and Pittsburgh.
Lucero, L.J., Fash, B.W. (Eds.), 2006. Precolumbian water management: ideology, ritual, and power. University of Arizona Press, Tucson.
Magnoni, A., Ardren, T., Hutson, S.R., Dahlin, B., 2014. Urban identities: social and spatial production at Classic period Chunchucmil, Yucatan, Mexico. In: Creekmore, A.T., Fisher, K.D. (Eds.), Making Ancient Cities. Cambridge University Press, Cambridge, pp. 145–180.
Magnoni, A., Hutson, S.R., Dahlin, B., 2012. Living in the city: settlement patterns and the urban experience at Classic period Chunchucmil, Yucatan, Mexico. Ancient Mesoamerica 23, 313–343. https://doi.org/10.1017/S0956536112000223.
Magnoni, A., Stanton, T.W., Barth, N., Fernández-Díaz, J.C., Osorio León, J.F., Pérez Ruíz, F., Wheeler, J.A., 2016. Detection thresholds of archaeological features in airborne Lidar data from central Yucatán. Adv. Archaeol. Pract.: A J. Soc. Am. Archaeol. 4, 232–248. https://doi.org/10.7183/2326-3768.4.3.232.
Maler, T., 1997. Península Yucatán, Monumenta American Vol. 5 Mann Verlag, Berlin, Gebr.
Marken, D.B., Fitzsimmons, J.L. (Eds.), 2015. Classic Maya polities of the Southern Lowlands: integration, interaction, dissolution. University Press of Colorado, Boulder.
Martos López, L.A., 2009. The discovery of Plan de Ayutla, Mexico. In: Golden, C., Houston, S., Skidmore, J. (Eds.), Maya Archaeology 1. Precolumbia Meso Press, San Francisco, pp. 60–75.
Masini, N., Coluzzi, R., Lasaponara, R., 2011. On the Airborne Lidar Contribution in Archaeology: from Site Identification to Landscape Investigation. In: Wang, C.-.C. (Ed.), Laser Scanning: Theory and Applications. IntechOpen, London, pp. 263–290.
Masson, M.A., Peraza Lope, C., 2014. Kukulcan's realm: urban life at ancient Mayapán. The University Press of Colorado, Boulder.
Mayer, K.H., 2006. The Maya ruins of Primera Sección, Chiapas, Mexico. Mexicon 28, 63–66.
McClung de Tapia, E., 1992. The origins of plant cultivation in Mesoamerica and Central America. In: Cowan, C.W., Watson, P.J. (Eds.), The Origins of Agriculture. An International Perspective, pp. 143–172.
McFarland, J., Cortes-Rincon, M., 2019. Mapping Maya Hinterlands: LiDAR Derived Visualization to Identify Small Scale Features in Northwestern Belize. Humboldt Journal of Social Relations 1, 13.
McKee, B.R., Sever, T.L., Sheets, P.D., 1994. Prehistoric footpaths in Costa Rica: remote sensing and field verification. In: Sheets, P.D., McKee, B.R. (Eds.), Archaeology, Volcanism, and Remote Sensing in the Arenal Region, Costa Rica. University of Texas Press, Austin, pp. 142–157.
Megarry, W.P., Davenport, B.A., Comer, D.C., 2016. Emerging Applications of LiDAR / Airborne Laser Scanning in the Management of World Heritage Sites. Conservation and Management of Archaeological Sites 18, 393–410. https://doi.org/10.1080/13505033.2016.1290481.
Morales López, A., Folan, W.J., 2005. Santa Rosa Xtampak, Campeche: su patrón de asentamiento del Preclásico al Clásico. Mayab 18, 5–16.
Murtha, T., Golden, C., Cyphers, A., 2018. Beyond Inventory and Mapping: LIDAR, Landscape and Digital Landscape Architecture. Journal of Digital Landscape Architecture 3, 249–259.
Murtha, T.M., 2015. Negotiated landscapes: comparative settlement ecology of Tikal and Caracol. In: Marken, D., Fitzpatrick, J. (Eds.), Ancient Maya Polities. University Press of Colorado, Boulder, pp. 75–98.
Murtha, T.M., 2009. Land and labor: Classic Maya agriculture at Caracol. Belize. VDM Verlag Dr, Müller, Berlin.
Murtha, T.M., Broadbent, E.N., Golden, C., Scherer, A.K., Schroder, W., Wilkinson, B., Almeyda Zambrano, A., 2019a. Drone-mounted Lidar survey of Maya settlement and landscape. Latin American Antiquity 30, 630–636. https://doi.org/10.1017/laq.2019.51.
Murtha, T.M., Lawres, N., Mazurczyk, T., Brown, M., 2019b. Investigating the role of archaeological information and practice in landscape conservation design and planning in North America. Adv. Archaeol. Pract.: A J. Soc. Am. Archaeol. 7, 382–394. https://doi.org/10.1017/aap.2019.32.
Neff, L.T., 2008. A study of agricultural intensification: ancient Maya agricultural terracing in the Xunantunich hinterland, Belize, Central America (Unpublished PhD dissertation). University of Pennsylvania, Philadelphia.
Nondédéo, P., Arnauld, M.C., Michelet, D., 2013. Río Bec settlement patterns and local sociopolitical organization. Ancient Mesoamerica 24, 373–396. https://doi.org/10.1017/S0956536114000017.
O'Donnell, M.S., Ignizio, D.A., 2012. Bioclimatic predictors for supporting ecological applications in the conterminous United States, Data Series 691. U.S, Geological Survey, Reston, VA.
Palka, J., 2001. Ancient Maya defensive barricades, warfare, and site abandonment. Latin American Antiquity 12, 427–430. https://doi.org/10.2307/972088.
Parsons, J.R., 1990. Critical reflections on a decade of full-coverage regional survey in the Valley of Mexico. In: Fish, S.K., Kowalewski, S.A. (Eds.), The Archaeology of Regions: A Case for Full-Coverage Survey. Smithsonian Institute Press, Washington, DC, pp. 7–32.
Piña Chan, R., 1959. Atlas arqueológico de la República Mexicana: Chiapas. Instituto Nacional de Antropología e Historia, Mexico City.
Pingel, T.J., Clarke, K., Ford, A., 2015. Bonemapping: a Lidar processing and visualization technique in support of archaeology under the canopy. Cartography and Geographic Information Science 42, S18–S26. https://doi.org/10.1080/15230406.2015.1059171.
Piperno, D.R., Ranere, A.J., Holst, I., Iriarte, J., Dickau, R., 2009. Starch grain and phytolith evidence for early ninth millennium B.P. maize from the Central Balsas River Valley. Mexico. PNAS USA 106, 5019–5024.
Plog, S., 1990. Agriculture, sedentism and environment in the evolution of political systems. In: Upham, S. (Ed.), The Evolution of Political Systems. Cambridge University Press, Cambridge, pp. 177–199.
Pollock, H.E.D., Roys, R.R., Proskouriakoff, T., Ledyard Smith, A., 1962. Mayapan, Yucatan, Mexico, Publication 619. Carnegie Institution of Washington, Washington, DC.
Puleston, D.E., 1973. Ancient Maya settlement patterns and environment at Tikal, Guatemala: implications for subsistence models (Unpublished. PhD dissertation). University of Pennsylvania.
Reese-Taylor, K., Hernández, A.A., Esquivel, F.C.A.F., Monteleone, K., Uriarte, A., Carr, C., Acuña, H.G., Fernández-Diaz, J.C., Peuramaki-Brown, M., Dunning, N., 2016. Boots on the Ground at Yaxnohcah: Ground-Truthing Lidar in a Complex Tropical Landscape. Adv. Archaeol. Pract.: A J. Soc. Am. Archaeol. 4, 314–338. https://doi.org/10.7183/2326-3768.4.3.314.
Rice, D.S., Rice, P.M., 1981. Muralla de Leon: a lowland Maya fortification. Journal of Field Archaeology 8, 271–288. https://doi.org/10.1179/009346981791505003.
Ricketson, O., Ricketson, E., 1937. Uaxactun, Guatemala, Group E, 1926–1937. Carnegie Institute of Washington, Washington, DC.
Risbøl, O., Gustavsen, L., 2018. LiDAR from drones employed for mapping archaeology – potential, benefits, and challenges. Archaeological Prospection 25, 329–338. https://doi.org/10.1002/arp.1712.
Roberts, P., Hunt, C., Arroyo-Kalin, M., Evans, D., Boivin, N., 2017. The deep human prehistory of global tropical forests and its relevance for modern conservation. Nat. Plants 3, 17093.

de Robina, R., 1956. Estudio preliminar de las ruinas de Hochob, Municipio de Hopelchen. Campeche, Editorial Atenea, Mexico City.
Rosenswig, R.M., López-Torrijos, R., Antonelli, C.E., Mendelsohn, R.R., 2013. Lidar mapping and surface survey of the Izapa state on the tropical piedmont of Chiapas, Mexico. J. Archaeol. Sci. 40, 1493–1507.
Ruhl, T., Dunning, N.P., Carr, C., 2018. Lidar reveals possible network of ancient Maya marketplaces in southwestern Campeche, Mexico. Mexicon 40, 83–91.
Sanders, W.T., 1999. Three valleys: twenty-five years of settlement archaeology in Mesoamerica. In: Billman, B.R., Feinman, G.M. (Eds.), Settlement Pattern Studies in the Americas: Fifty Years since Virú. Smithsonian Institution Press, Washington, DC, pp. 12–21.
Sanders, W.T., 1977. Environmental heterogeneity and the evolution of lowland Maya civilization. In: Adams, R.E.W. (Ed.), The Origins of Maya Civilization. University of New Mexico Press, Albuquerque, pp. 287–297.
Sanders, W.T., 1973. The cultural ecology of the lowland Maya: a reevaluation. In: Culbert, T.P. (Ed.), The Classic Maya Collapse. University of New Mexico Press, Albuquerque, pp. 325–365.
Sanders, W.T., 1963. Cultural ecology of the Maya lowlands, Part 2. Estudios de Cultura Maya 3, 203–241.
Sanders, W.T., 1962. Cultural ecology of the Maya lowlands, Part 1. Estudios de Cultura Maya 2, 79–121.
Sanders, W.T., Santley, R.S., 1983. A tale of three cities: energetics and urbanization in pre-hispanic Central Mexico. In: Vogt, E.Z., Leventhal, R. (Eds.), Prehistoric Settlement Patterns: Essays in Honor of Gordon R. University of New Mexico Press, Albuquerque, Willey, pp. 243–291.
Scarborough, V.L., 2003. The flow of power: ancient water systems and landscapes. School of American Research, Santa Fe.
Scarborough, V.L., 1998. Ecology and ritual: water management and the Maya. Latin American Antiquity 9, 135–159.
Scarborough, V.L., Chase, A.F., Chase, D.Z., 2012a. Low-Density Urbanism, Sustainability, and IHOPE-Maya: Can the Past Provide More than History? UGEC Viewpoints 8, 20–24.
Scarborough, V.L., Dunning, N.P., Tankersley, K.B., Carr, C., Weaver, E., Grazioso, L., Lane, B., Jones, J.G., Buttles, P., Valdez, F., 2012b. Water and sustainable land-use at the ancient tropical city of Tikal, Guatemala. Proc. Natl. Acad. Sci. 109, 12408–12413. https://doi.org/10.1073/pnas.1202881109.
Scherer, A.K., Golden, C.W., 2009. Tecolote, Guatemala: archaeological evidence for a fortified Late Classic Maya political border. Journal of Field Archaeology 34, 285–305. https://doi.org/10.1179/009346909791070907.
Schroder, W., Golden, C., Scherer, A., Murtha, T., Alcover Firpi, O., 2019. Remote sensing and reconnaissance along the Lacantún river: the Lakamtuun dynasty and the sites of El Palma and Benemérito de las Américas, Primera Sección. Mexicon 41, 157–167.
Schroder, W., Golden, C.W., Scherer, A.K., Jiménez Álvarez, S. del P., Dobereiner, J., Méndez Cab, A., 2017. At the crossroads of kingdoms: recent investigations on the periphery of Piedras Negras and its neighbors. The PARI Journal 17, 1–15.
Sheets, P., Hoopes, J., Melson, W., McKee, B., Sever, T., Mueller, M., Chenault, M., Bradley, J., 1991. Prehistory and Volcanism in the Arenal Area, Costa Rica. Journal of Field Archaeology 18, 445–465. https://doi.org/10.2307/530407.
Sheets, P., Sever, T., 1988. High-Tech Wizardry. Archaeology 41, 28–35.
Sheets, P.D., 1991. "Very-to-Barely" Remote Sensing of Prehistoric Features under Tephra in Central America. In: Behrens, C.A., Sever, T.L. (Eds.), Applications of Space-Age Technology in Anthropology: November 28, 1990 Conference Proceedings. NASA Science and Technology Laboratory John C, Stennis Space Center, Mississippi, pp. 167–180.
Stanton, T.W., Ardren, T., Barth, N.C., Fernández-Díaz, J.C., Rohrer, P., Meyer, D., Miller, S.J., Magnoni, A., Pérez, M., 2020. 'Structure' density, area, and volume as complementary tools to understand Maya settlement: an analysis of Lidar data along the great road between Coba and Yaxuna. J. Archaeolog. Sci.: Rep. 29. https://doi.org/10.1016/j.jasrep.2019.102178.
Tarazona de González, S.G., Kurjack, E.B., 1980. Atlas arqueológico del Estado de Yucatán. SEP, Instituto Nacional de Antropología e Historia, Centro Regional del Sureste, Mexico City.
Terrenato, N., Ammerman, A.J., 1996. Visibility and site recovery in the Cecina Valley Survey, Italy. Journal of Field Archaeology 23, 91–109. https://doi.org/10.1179/009346996791973990.
Tovalín, A., Ortiz, V., 2005. El sitio arqueológico de la Primera Sección de Benemérito de las Américas, Chiapas. Arqueología 35, 33–49.
Turner II, B.L., 1974. Prehistoric intensive agriculture in the Mayan lowlands. Science 185, 118–124. https://doi.org/10.1126/science.185.4146.118.
Underhill, A., Feinman, G.M., Nicholas, L., Bennett, G., Fang, H., Luan, F., Yu, H., Cai, F., 2002. Regional survey and the development of complex societies in southeastern Shandong, China. Antiquity 76, 745–755. https://doi.org/10.1017/S0003598X00091195.
VanValkenburgh, P., Cushman, K.C., Castillo Butters, L.J., Rojas Vega, C., Roberts, C.B., Kepler, C., Kellner, J., 2020. Lasers without lost cities: using drone Lidar to capture architectural complexity at Kuelap, Amazonas, Peru. Journal of Field Archaeology 45, S75–S88. https://doi.org/10.1080/00934690.2020.1713287.
von Schwerin, J., Richards-Rissetto, H., Remondino, F., Spera, M.G., Auer, M., Billen, N., Loos, L., Stelson, L., Reindel, M., 2016. Airborne LiDAR acquisition, post-processing and accuracy-checking for a 3D WebGIS of Copan, Honduras. J. Archaeolog. Sci.: Rep. 5, 85–104. https://doi.org/10.1016/j.jasrep.2015.11.005.
Webster, D., Murtha, T.M., Straight, K.D., Silverstein, J., Martinez, H., Terry, R.E., Burnett, R., 2007. The great Tikal earthwork revisited. Journal of Field Archaeology 32, 41–64. https://doi.org/10.1179/009346907791071700.
Wilkinson, T.J., 2000. Regional approaches to Mesopotamian archaeology: the contribution of archaeological surveys. J. Archaeol. Res. 8, 219–267. https://doi.org/10.1023/A:1009487620969.
Witschey, W.R.T., Brown, C., 2010. The electronic atlas of Maya sites [WWW Document]. URL http://mayagis.smv.org/google_earth_data.htm (accessed 3.15.16).
Yaeger, J., Brown, M.K., Cap, B., 2016. Locating and Dating Sites Using Lidar Survey in a Mosaic Landscape in Western Belize. Adv. Archaeol. Pract.: A J. Soc. Am. Archaeol. 4, 339–356. https://doi.org/10.7183/2326-3768.4.3.339.
Zakšek, K., Oštir, K., Kokalj, Ž., 2011. Sky-view factor as a relief visualization technique. Remote Sens. 3, 398–415. https://doi.org/10.3390/rs3020398.